Geochemistry of the northern Cache Creek terrane and implications for accretionary processes in the Canadian Cordillera

Joseph M. English, Mitchell G. Mihalynuk, and Stephen T. Johnston

Abstract: The northern Cache Creek terrane in the Canadian Cordillera includes a subduction complex that records the existence of a late Paleozoic – Mesozoic ocean basin and provides an opportunity to assess accretionary processes that involve the transfer of material from a subducting plate to an upper plate. Lithogeochemical data from basaltic rocks indicate that the northern Cache Creek terrane is dominated by two different petrogenetic components: (1) a dominant suite of subalkaline intrusive and extrusive rocks mostly of arc affinity and (2) a volumetrically less significant suite of alkaline volcanic rocks of within-plate affinity. The subalkaline intrusive and extrusive rocks constitute a section of oceanic lithosphere that is interpreted to have occupied a fore-arc position during the Late Triassic and Early Jurassic before it was accreted during collisional orogenesis in the Middle Jurassic. Alkaline volcanic rocks in the northern Cache Creek terrane are stratigraphically associated with carbonate strata that contain Tethyan fauna that are exotic with respect to the rest of North America; together, they are interpreted as remnants of oceanic seamounts and (or) plateaux. The volcanic rocks are a minor component of the carbonate stratigraphy, and it appears that the majority of the volcanic basement was either subducted completely at the convergent margin or underplated at greater depth in the subduction zone. In summary, accretion in the northern Canadian Cordillera occurred principally by the accretion of island arcs and emplacement of fore-arc ophiolites during collisional orogenesis. The transfer of oceanic sediments and the upper portions of oceanic seamounts from the subducting plate to an accretionary margin accounts for only small volumes of growth of the upper plate.

Résumé : French French

[Traduit par la Rédaction]

Received 9 April 2009. Accepted 16 November 2009. Published on the NRC Research Press Web site at cjes.nrc.ca on .

Paper handled by Associate Editor M. Colpron.

J.M. English[1,2] and S.T. Johnston. School of Earth and Ocean Sciences, University of Victoria, P.O. Box 3055 STN CSC, Victoria, BC V8W 3P6, Canada.
M.G. Mihalynuk. British Columbia Ministry of Energy and Mines, P.O. Box 9320, Stn Prov Govt, Victoria, BC V8W 9N3, Canada.

[1]Corresponding author (e-mail: dr.joe_english@yahoo.ca).
[2]Present address: Petroceltic International, Styne House, Upper Hatch Street, Dublin 2, Ireland.

Introduction

Accretionary processes involve the transfer of material such as oceanic sediments, seamounts, island arcs, oceanic plateaux, and microcontinental fragments from a subducting plate to an upper plate. Evidence of accretion tectonics can be observed at many of the world's active continental margins as well as along the suture zones of ancient orogenic belts, and this process is an important mechanism for continental growth. Accretion occurs by two principal mechanisms: (1) accretion of island arcs as a continental plate enters and blocks up a subduction zone (e.g., the Banda Arc is currently being thrust onto the continental margin of Australia at Timor Island), and (2) transfer of oceanic sediments, seamounts, and ridges from the subducting plate and incorporation into the subduction complex (Cloos 1993). The northern Cache Creek terrane in the Canadian Cordillera includes a subduction complex that records the existence of a late Paleozoic – Mesozoic ocean basin (Monger 1975; Cordey et al. 1991; Orchard 1991; Fig. 1) and hence provides an opportunity to assess the preservation–accretion potential of various tectonic elements within the oceanic realm.

The objectives of this paper are to (1) elucidate the original tectonic setting(s) in which the mafic rocks of the northern Cache Creek terrane were produced, and (2) discuss the significance of the northern Cache Creek terrane as an analogue for accretionary processes.

Geological background

The Cache Creek terrane is a belt of Mississippian to Lower Jurassic oceanic rocks (Monger 1975; Cordey et al. 1991; Orchard 1991) that occupies a central position within the Intermontane Belt of the Canadian Cordillera in British Columbia (Coney et al. 1980; Fig. 1). Fossil fauna within carbonate rocks of the Cache Creek terrane are uniquely exotic with respect to the remainder of the Canadian Cordillera, as they are typical of the equatorial Tethyan realm, contrasting with coeval faunas in adjacent arc terranes of Stikinia and Quesnellia (Fig. 1) that show closer linkages with ancestral North America (Monger and Ross 1971; Orchard et al. 2001). Rocks composing the Cache Creek terrane represent two distinctive lithotectonic elements: a Middle Triassic to Early Jurassic, subduction-related accretionary complex, and a dismembered oceanic basement assemblage (Terry 1977; Monger et al. 1982; Ash 1994; Mihalynuk 1999). In map view, the northern Cache Creek terrane (north of 58°) is a southeastward-tapering wedge (Fig. 1); this terrane is composed of tectonically imbricated slices of chert, argillite, volcaniclastic rocks, carbonate, and wacke, with a belt of ultramafics, gabbro, and basalt along its western margin, which is demarked by the crustal-scale Nahlin Fault (Aitken 1959; Mihalynuk et al. 2002, 2003*a*; Figs. 1, 2). Rocks of the northern Cache Creek terrane were emplaced to the west over the Stikine terrane in the Middle Jurassic, resulting in fold-and-thrust belt formation in the Whitehorse Trough (Thorstad and Gabrielse 1986; Mihalynuk 1999; English et al. 2005; English and Johnston 2005); the timing of this deformational event is constrained to be younger than the age of the youngest blueschist in the Cache Creek terrane (French Range, ~174 Ma, Mihalynuk et al. 2004*a*) and older than the age of the oldest postdeformational intrusions (~172 Ma, Mihalynuk et al. 1992, 2003*a*; Bath 2003). Postcollisional chert–pebble conglomerates derived from the Cache Creek terrane were deposited across the Whitehorse Trough and Bowser Basin of the Stikine terrane during Bajocian time (Ricketts et al. 1992; Mihalynuk et al. 2004*a*), providing an overlap assemblage.

Geology of the Nakina area

Cache Creek terrane occurs within the relatively poorly exposed central plateau region of the Canadian Cordillera. Arguably, the best exposures of Cache Creek terrane are in northern British Columbia where the plateau margin is deeply incised by the Nakina River and its tributaries. Northern Cache Creek terrane rocks of the Nakina River area (Fig. 1) can be assigned to one of five generalized units: (1) mantle, (2) mafic intrusive, (3) mafic volcanic, (4) hemipelagite–siliciclastic, and (5) carbonate (Fig. 2). A separate mafic volcanic unit with sparse relict pillows is known as the Yeth Creek formation (informal, Mihalynuk et al. 2004*b*), which crops out south of the Nahlin Fault (Fig. 1). A number of postdeformational Middle Jurassic quartz-dioritic to granodioritic plutons intrude the Cache Creek terrane within the study area (Fig. 2). Metamorphic grade of the Nakina River area is typically prehnite–pumpellyite to pumpellyite–actinolite facies, although thermal upgrading to biotite grade is observed around large plutons.

Mantle rocks

Tectonized harzburgite, composed of olivine and orthopyroxene with accessory clinopyroxene and chromite, forms a coherent 1.5 km × 15 km, dun-weathering body along the southwestern margin of the Cache Creek terrane (Fig. 2). Elongate clusters of orthopyroxene and chromite grains outline a relict fabric interpreted as having a high-temperature mantle origin (e.g., Nicolas and Violette 1982; Nicolas 1995); lineated orthopyroxene grains are up to 2 cm in length. This fabric is cut by undeformed ~2–4 mm thick pyroxenite dikelets. No deformational fabrics postdate the pyroxenite dikelets, indicating that the harzburgite acted as a rigid body during emplacement. Where serpentinized, much younger creep has caused disruption of Cretaceous dikes (~138 Ma, M. Villeneuve, written communication, 2004) and Recent modification of the Quaternary landscape. However, most structural disaggregation of serpentinized harzburgite predates intrusion of Middle Jurassic plutons. Such is the case within the western part of a serpentinite mélange belt north of the Nakina River, where harzburgite forms the dominant exotic block type.

The age of the ultramafic rocks remains unconstrained: an Early Triassic U/Pb zircon age of 245.4 ± 0.8 Ma has been reported from an isolated peridotite body in the northeastern part of the Cache Creek terrane (Gordey et al. 1998). The relationship between this peridotite body and the ultramafic rocks described here is unknown.

Mafic intrusive rocks

Medium-grained plagioclase and pyroxene gabbro and amphibole-phyric diorite occur as isolated intrusions and as blocks within serpentinite mélange where they increase in

Fig. 1. Map of British Columbia showing the distribution of the primary components of the Intermontane Belt in the northern Canadian Cordillera (top right) and a regional geologic map (main). This geology map does not include post-Middle Jurassic rock units. The Nakina area is outlined by a box with broken lines.

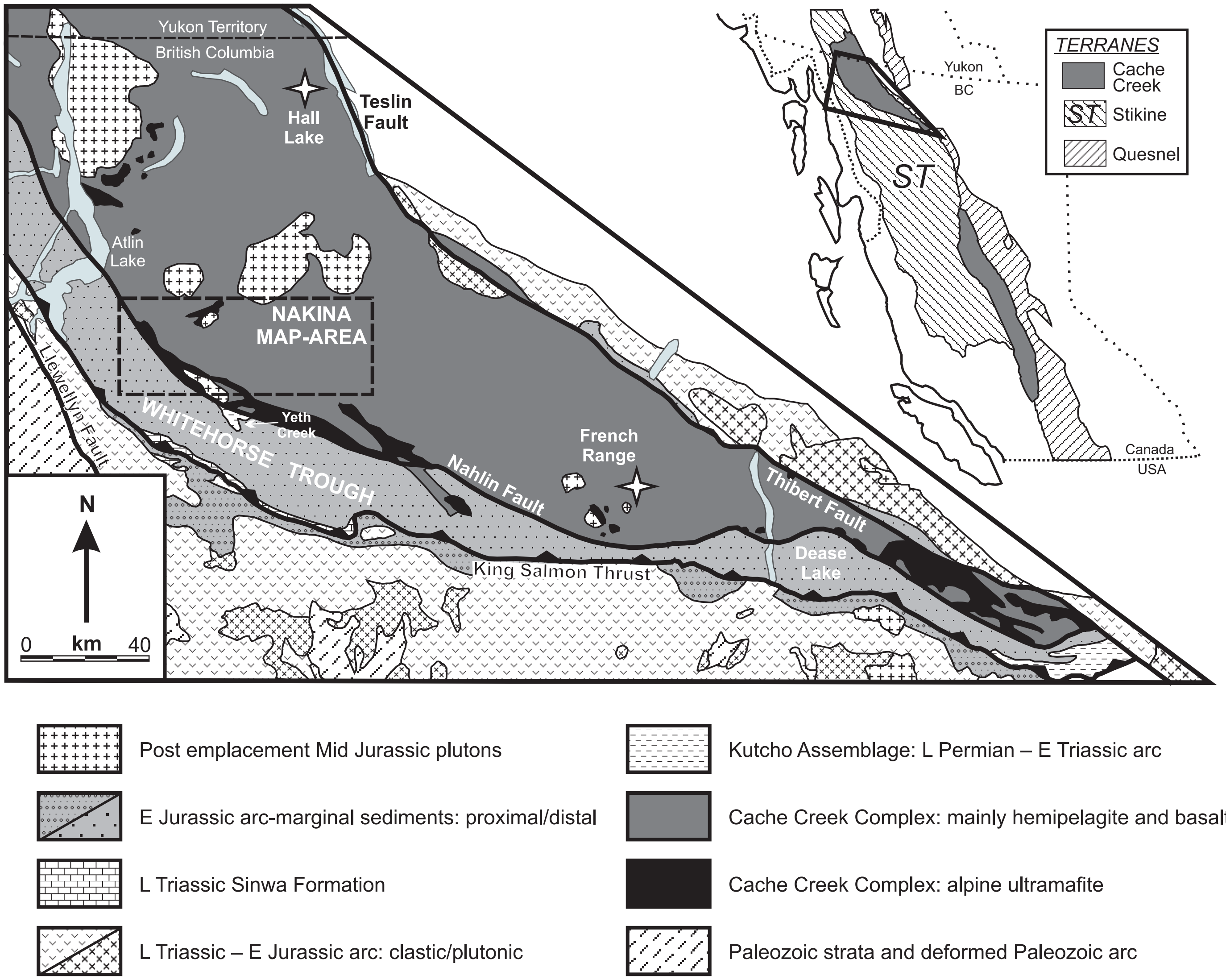

abundance to the east but are subordinate to the harzburgite. Primary clinopyroxene is subhedral to euhedral and commonly displays exsolution lamellae and zoning. In more altered samples, especially within the serpentinite mélange belt, primary pyroxene and hornblende are preferentially altered to actinolite; secondary minerals mainly form pseudomorphs after the igneous minerals that they replaced. Plagioclase is variably altered, from fresh to totally turbid; authigenic minerals include white mica, prehnite, quartz, and carbonate. Pyroxene–hornblende is subequal in abundance to plagioclase. Ophitic textures are common.

Some of these intrusive rocks are intensely sheared, while others are undeformed. A folded, sheetlike gabbroic body displays an intrusive contact with overlying mafic volcanic rocks and fault contact with underlying ultramafic, mafic, and quartz-rich clastic rocks south of Mount O'Keefe. Gabbroic rocks in the Hard Luck Peaks area display an intrusive contact with basaltic rocks. Hornblende-phyric diorite, gabbro, and tonalite blocks within the serpentinite mélange belt range in size from 1 m to hundreds of metres and are undeformed compared with the serpentinite matrix. Tonalite and quartz–diorite blocks from the serpentinite mélange have yielded Middle–Late Permian ages (Devine 2002; samples FDE01-31-7 and FDE01-31-12, Fig. 3).

In the southeastern part of the study area, diorite is intruded by an irregular network of comagmatic pegmatitic tonalite dykes <0.5 m thick. These tonalite dykes are composed of plagioclase and hornblende with $\sim$10% interstitial quartz and accessory titanite and zircon. Plagioclase has been partially altered to prehnite, whereas hornblende only displays traces of chlorite alteration. A $^{40}Ar/^{39}Ar$ age determination of 265 ± 25 Ma (Mihalynuk et al. 2003*a*) using laser step-heating analysis on the hornblende is consistent with that of extracted zircons that reveal a Late Permian U/Pb age (261.4 ± 0.3 Ma, Mihalynuk et al. 2003*a*; sample MMI01-27-6, Fig. 3). This age is consistent

Fig. 2. Generalized bedrock geology map of the northern Cache Creek terrane in the Nakina map area with a 10 km North American datum (NAD) 83 Universal Transverse Mercator (UTM) grid superimposed (National Togographic System (NTS) 104N/1, 2, and 3). Mt, Mount; Mtn, Mountain.

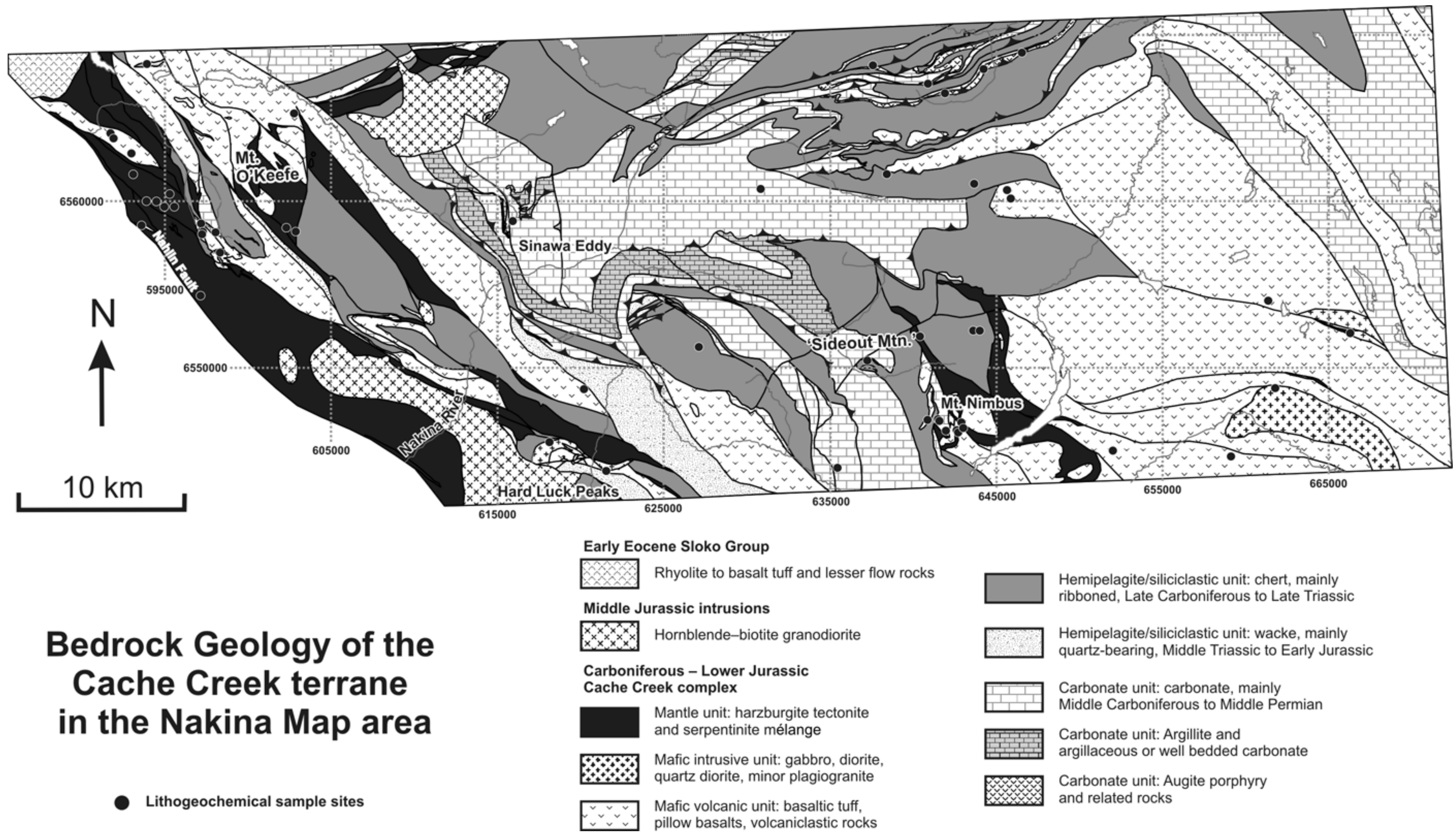

Fig. 3. Schematic stratigraphic sections from the Nakina River area of the Cache Creek terrane. Note that all broken lines between units represent mappable faults. The oceanic crustal assemblage is Permian in age based on magmatic U–Pb dating from samples from Hard Luck Peaks and Mt. Nimbus. A quartz-rich clastic unit unconformably overlying the oceanic crustal assemblage at Hard Luck Peaks is characterized by Early Triassic detrital ages, overlapping with published ages from the Kutcho assemblage. In the Sideout Mtn. area, Upper Mississippian carbonate lies in conformable contact with alkaline volcanic rocks that are older than the mafic rocks of the oceanic crustal assemblage. M, melange; SM, serpentinite melange; Mt, Mount; Mtn, Mountain.

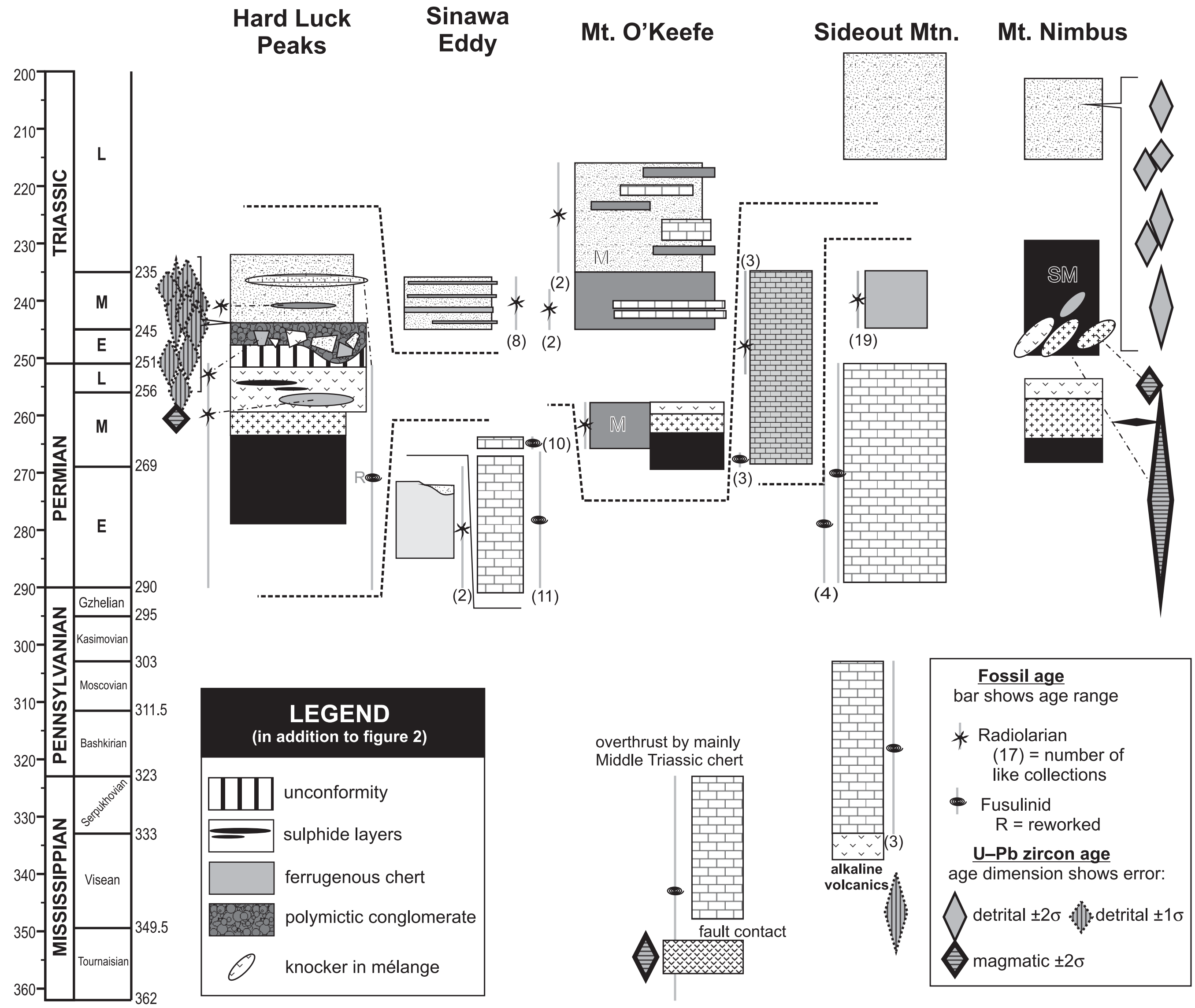

with U–Pb zircon ages of magmatic blocks within the serpentinite mélange (255 ± 2.8 and 275 ± 17 Ma, Devine 2002). Correlative rocks in the southern Cache Creek terrane are the same age as the tonalite (within the limits of error: 257 ± 5 Ma, Schiarizza et al. 2000). Hence, it appears that the felsic magmatism evident in the oceanic crust is of Middle to Late Permian age (Fig. 3).

Mafic volcanic rocks

Basalt and mafic volcaniclastic rock is the dominant volcanic lithology. This unit commonly displays well-preserved, aphanitic lapilli and ash-sized fragments despite widespread replacement by prehnite, pumpellyite, calcite, and chlorite. Fresh surfaces are a distinctive mint green colour with a grey or pinkish hue caused by filaments (fine shear bands) of clay and iron oxides. Weathered surfaces display a fragmental texture with angular clasts up to 10 cm in size; these clasts commonly contain relict plagioclase and pyroxene phenocrysts. Both the pyroxene and plagioclase range from fresh to extensively altered in thin section. Locally, pyroxene phenocrysts are euhedral. Disseminated pyrite, pyrhhotite, and minor chalcopyrite are common, but compose <1%–2% of the unit. Interbeds of chert are Middle Triassic in the northern part of the Nakina area (Mihalynuk et al. 2003*a*) and Permian in the Hard Luck Peaks area (Mihalynuk et al. 2003*b*; Fig. 3). Extensive exposures of well-formed pillows near Hard Luck Peaks are fine-grained, vesicular, and in some cases contain medium-grained feldspar laths composing up to 10% of the rock.

Hemipelagite–sSiliciclastic rocks

Chert, argillite, and fine-grained wacke that are the predominant lithology throughout most of the Cache Creek terrane are roughly equally abundant as basalt and limestone in the Nakina area. Chert and argillaceous chert vary in colour from black to grey to tan and occur as either massive, featureless successions or well-ribboned with alternating 2–6 cm thick beds of chert and 2–5 mm beds of dark grey argillite. Chert is also commonly interbedded with mafic volcaniclastic strata or wacke containing a large proportion of volcanic quartz grains. Radiolaria extracted from chert in the Nakina area range in age from Permian to Late Triassic (Mihalynuk et al. 2003*a*; Fig. 3); elsewhere in the northern Cache Creek terrane, radiolaria range in age from Carboniferous to Early Jurassic (Cordey et al. 1991).

Siliceous mud-rich wacke in the Nakina area is brown and less commonly dark grey, black or blue-grey. This wacke commonly contains chert grains, rare cobbles, and volcanic clasts from ash to lapilli size. Sparse quartz grains may be derived from quartz diorite, clasts of which occur as rare, foliated granules. Locally, these strata grade into chert or volcaniclastic rocks. Some wacke units are dominated by sand or silt-sized grains. Detrital zircons from wacke in the Nakina area are as young as Early Jurassic (182 ± 4 Ma, Mihalynuk et al. 2003*a*) although most detrital ages are Middle to Late Triassic in age (e.g., 206–241 Ma, Devine 2002; with one ~330–~345 Ma population, Mihalynuk et al. 2003*a*; Fig. 3).

In comparison, granitoid clasts within the Whitehorse Trough are typically of Late Triassic age where they have been studied in the Yukon (e.g., 216–207 Ma, Hart 1996; Johannson et al. 1997) and are lithologically similar to intrusive bodies within Stikine and Quesnel terranes. Volcanic clasts range from Late Triassic to Early Jurassic age with a major influx of clasts and tuff of probable Nordenskiold dacite affinity (Johannson et al. 1997; 188–183 Ma, Colpron and Friedman 2008; D. Canil, personal communication, 2007).

Carbonate rocks

Carbonate rocks compose much of the central part of the Nakina area (Fig. 2). Typical lithologies include light grey, well-bedded, bioclastic (turbiditic?) limestone; coarse limestone breccia which occurs as sheets and channels decimetres to several metres thick; indistinctly thick- to medium-bedded, cream-coloured limestone 80–120 m thick; and distinctly medium- to thin-bedded, dark grey to black, fetid and (or) argillaceous limestone ~40 m thick.

Massive limestone is the most abundant unit; and many cubic kilometres are featureless except for sparse crinoid ossicles and fragments of bivalves, bryozoa, rare corallites, pisoids or limestone clasts. Massive limestone probably accumulated in an intraoceanic platformal setting during Late Carboniferous and Permian time and interfingered with well-bedded lagoonal facies and talus to turbidite facies on the platform margins (Monger 1975; Merran 2002; Mihalynuk et al. 2003*a*).

Isolated volcanic accumulations occur within carbonate units. Volcanic flows and flow breccias form the substrate of some carbonate reefs (Merran 2002; English et al. 2002). Flows are brown weathering and pinkish maroon fresh, with pillows containing zones of elongate, calcite-filled vesicles and separated by interpillow hyaloclastite. Rounded to angular carbonate blocks compose irregular interlayers within the flows; they are interpreted to be of olistostromal origin. The most extensive framework reef constructed on an accumulation of volcanic rocks occurs on the southwest flank of “Sideout Mountain” (Figs. 2, 3; Monger 1977; Merran 2002), where Upper Mississippian reef – lagoonal carbonates overlie volcanic breccia.

Feldspar porphyry, in assumed stratigraphic contact with overlying Carboniferous well-bedded limestone, occurs as pillowed flows and volcaniclastic layers <10 m thick. An augite porphyry unit (Fig. 2) occurs as a laterally extensive, monomictic matrix-supported breccia reaching up to 250 m in thickness. It contains blocks that are up to 1 m across. Interlayered augite crystal tuffs contain up to 30% zoned euhedral crystals up to 1 cm across, as well as less abundant plagioclase crystals. Groundmass is dominated by plagioclase and iron oxides. This unit grades upwards into limestone.

Yeth Creek formation

In the Yeth Creek area (Fig. 1), basalt southwest of the Nahlin Fault is juxtaposed with ultramafite across to the northeast. Dark green to grey, fine-grained, pyroxene and plagioclase-phyric vesicular pillow basalts, breccia, and sheet flows are the principal lithologies. Plagioclase crystals are moderately altered by prehnite and pumpellyite (Fig. 4), and pyroxene crystals are fresh; prehnite–pumpellyite represents a metamorphic facies commonly displayed in mafic volcanic rocks of the Cache Creek terrane.

Occurrence of the Yeth Creek basalt southwest of the Nahlin fault is intriguing because, at the latitude of the Nakina area elsewhere, the Nahlin Fault marks the southwestern limit of the Cache Creek terrane. We tentatively include the Yeth Creek basalt with the Cache Creek terrane and interpret them as basement to the overlying siliciclastic sedimentary rocks of the Laberge Group in the Whitehorse Trough (Souther 1971). This stratigraphic relationship was not confirmed, but the basalt was sampled for lithogeochemical comparison with other basalts within the Cache Creek terrane.

Composition of mafic rocks

Methods

Representative samples from all of the mafic units described previously were selected for lithogeochemical analysis. The primary goal of this geochemical analysis is to determine the magma source and, hence, the paleotectonic environment of the igneous rocks. The success of this analysis hinges on obtaining an original geochemical signature that has not been modified by subsequent hydrothermal alteration and metamorphism. Major elements, especially alkalis, should be considered mobile during alteration and metamorphism (e.g., Smith and Smith 1976), although major element compositional classifications can be compared with immobile element compositional classifications to test major element mobility. All but one of the low field-strength elements (LFSE: K, Rb, Cs, U, Pb, Ba, and Sr) should be considered mobile. Thorium (Th) is the only LFSE that can be considered immobile in most circumstances (e.g., Jenner

Fig. 4. Photomicrographs of Yeth Creek formation basalt (sample MMI-02-34-1). Note the fresh grey orthopyroxene (opx) phenocryst and the formation of prehnite–pumpellyite on the plagioclase feldspar (plag) phenocryst. PPL, xxx; XP, xxx.

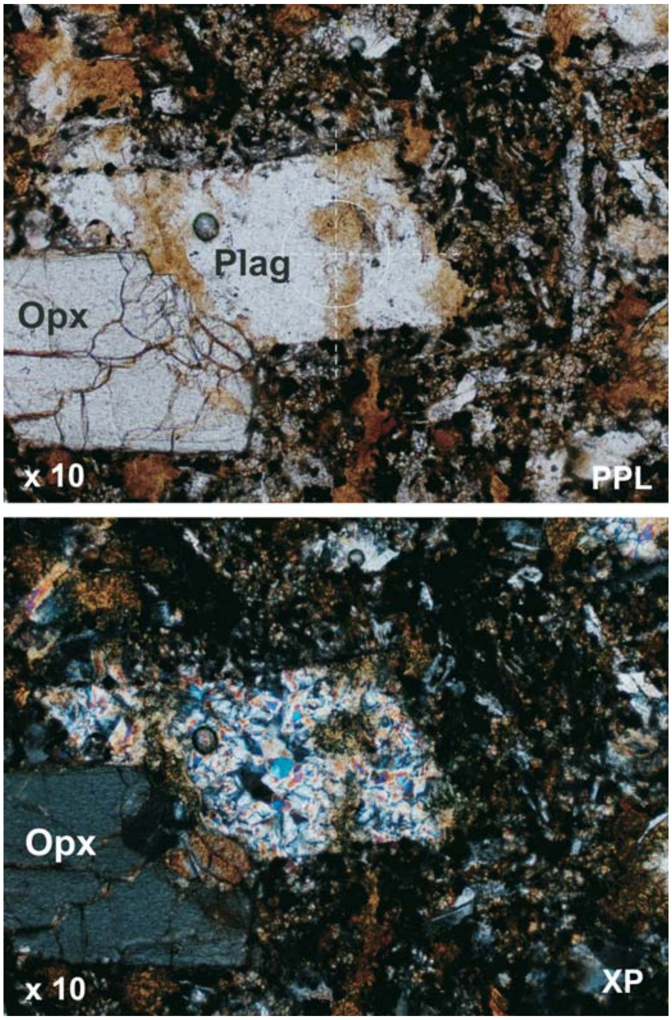

1996). High field-strength elements (HFSE) such as Ti, Zr, Hf, Nb, and Ta, and rare earth elements (REE) can be considered immobile in most cases (e.g., Jenner 1996) and, hence, they are the most reliable group of elements for determining paleotectonic environments. Discussions in this paper focus primarily on immobile element systematics.

Initially, samples of 18 intrusive and extrusive mafic rocks were selected for major- and trace-element analysis at ACME Analytical Laboratories in Vancouver, British Columbia (Table 1). This sample set includes samples from the mafic intrusive and volcanic units and from the volcanic rocks associated with the carbonate stratigraphy. Intrusive rock-sample selection was limited to isotropic gabbro samples so as to avoid cumulate layers. Thin-sections were cut for every sample to screen for high degrees of alteration or xenoliths that could not be detected in hand sample. Screened samples were prepared using steel jaw crusher and disk mill at the British Columbia Ministry of Energy and Mines rock preparation facility. Tungsten carbide grinding surfaces were not used to minimize trace-element contamination, particularly Ta and Nb. However, Cr contamination from the steel mill is a possibility, so we do not rely on Cr as a discriminant. Major oxides were determined by $LiBO_2$ fusion and inductively coupled plasma – emission spectrometry (ICP–ES) analysis, whereas minor- and trace-element – REE geochemistry were determined by inductively coupled plasma – mass spectrometry (ICP–MS) techniques. A blank and in-house standard reference material (SY-4 syenite) was carried through weighing, digestion, and analytical stages to monitor accuracy. For additional quality control, two blind repeat samples (with suffix "R") were submitted to assess precision (Table 1).

A second suite of 34 samples were selected for follow-up minor- and trace-element analysis at Memorial University in St. John's, Newfoundland (Table 2). These samples come from the same lithotectonic units that were sampled by the first suite; the purpose of this additional analysis was to build up a more statistically valid minor- and trace-element dataset on which to elucidate the petrogenetic origin of each of the mapped units. Once again, all samples were screened petrographically. The analytical procedure at Memorial University follows that of Jenner et al. (1990) where 0.1g of sample was subjected to a four acid attack (hydrofluoric, nitric, boric, and oxalic acids) and the solution was analyzed by ICP–MS using the method of standard addition to correct for matrix effects. For quality control, one geological reference standard (MRG-1 gabbro) was prepared and analyzed to assess accuracy, a reagent blank was run to measure the reagent contribution, and eight of the samples were analyzed in duplicate (with suffix "R") to assess precision (Table 2). At concentrations close to detection limit (Table 2), precision and accuracy are generally significantly poorer than at higher concentrations.

Geochemistry

On the basis of field-mapping criteria, rocks from the mafic intrusive and mafic volcanic units belong to an oceanic crustal assemblage. From a geochemical perspective, this oceanic crustal assemblage consists of island-arc tholeiites (IAT), island-arc calc-alkaline rocks, back-arc basin basalts (BABB), and enriched mid-ocean ridge basalts (E-MORB). Volcanic rocks interbedded with significant carbonate sections are ocean-island basalts (OIB) and more silica-rich alkaline volcanic rocks. Rocks that lie southwest of the terrane-bounding Nahlin Fault, the Yeth Creek formation, are BABB. The geochemical signature of each mapped lithotectonic unit is consistent between sample suites 1 and 2 that were analyzed at ACME Analytical Laboratories and Memorial University, respectively.

Analyzed samples from the Nakina area are both alkaline and subalkaline (Fig. 5A). Volcanic rocks interbedded with Carboniferous carbonate are classified as alkaline, and the remainder are subalkaline as demonstrated by the total alkalis versus silica (TAS) diagram of Cox et al. (1979). Most of the samples reveal a basaltic to basaltic andesite composition. Compositional groupings based on major-element profiles are consistent with those based on immobile trace-element compositions although classification varies slightly. For example, rock classification based on the TAS diagram compares well with that based on the immobile element Zr/TiO_2 versus Nb/Y diagram (Fig. 5B; Winchester and Floyd 1977). The only major difference between these plots is that

Table 1. Whole-rock major + minor elemental and rare-earth element abundances for mafic rocks in the Cache Creek terrane.

Sample:	FDE01-14-12	FDE01-23-6	FDE01-31-1a	FDE01-31-1b	FDE01-31-3	FDE01-31-4	FDE01-31-6	FDE01-31-7	FDE01-31-7R	FDE01-31-10	FDE01-31-12	JEN01-23-8
Lithology:	Augite-phyric tuff	Basalt	Basanite	Basanite	Basanite	Basalt	Gabbro	Gabbro	Gabbro	Volcani-clastic	Tonalite	Volcani-clastic
Unit:	Carbonate	Mafic volcanic	Carbonate	Carbonate	Carbonate	Mafic volcanic	Mafic intrusive	Mafic intrusive	Mafic intrusive	Mafic volcanic	Mafic intrusive	Mafic volcanic
Affinity:	OIB	IAT	OIB	OIB	OIB	E-MORB	IAT	IAT	IAT	BABB	Calc-alk	IAT
Easting:	640750	651840	641345	641345	641300	641880	642538	642538	642538	642711	642711	645368
Northing:	6567060	6544708	6546812	6546812	6546796	6546544	6546533	6546483	6546483	6546740	6546483	6560715
SiO_2	44.6	53.6	39.2	38.5	40.5	48.9	46.6	50.2	50.5	47.3	77.2	48.7
TiO_2	2.97	0.65	4.54	4.96	4.43	1.83	0.21	0.82	0.81	1.42	0.12	1.32
Al_2O_3	11.1	13.7	13.3	14.3	12.8	13.3	19.5	15.7	15.9	14.9	12.9	15.3
Fe2O3	11.4	8.6	12.2	12.9	11.6	10.8	5.4	9.1	9.0	11.2	0.2	10.5
MnO	0.13	0.14	0.17	0.16	0.13	0.17	0.1	0.13	0.13	0.17	<0.01	0.16
MgO	10.3	7.0	6.9	7.3	7.1	6.7	7.5	7.1	7.1	6.5	0.3	6.2
CaO	11.1	9.4	9.6	8.2	9.0	10.1	13.2	10.2	10.1	11.3	1.2	11.2
Na_2O	2.3	3.5	1.9	1.3	2.6	3.7	2.3	3.5	3.6	2.4	5.4	1.5
K_2O	1.0	0.1	1.9	2.3	1.6	0.1	0.5	0.0	0.1	0.3	1.5	0.3
P_2O_5	0.47	0.06	2.07	2.49	1.94	0.24	<0.01	0.06	0.06	0.09	<0.01	0.16
Cr_2O_3	0.074	0.04	0.011	0.017	0.012	0.012	0.017	0.005	0.005	0.016	0.008	0.013
LOI	4.4	3.2	7.6	6.8	7.2	4	4.8	3.1	2.7	4.6	0.9	4.7
C	0.64	0.11	0.71	0.28	0.76	0.25	<0.01	0.03	0.02	0.05	0.09	0.01
S	<0.01	0.02	<0.01	0.01	0.04	0.16	<0.01	0.01	<0.01	0.18	<0.01	0.02
Total	100.0	100.0	99.5	99.3	99.1	99.9	100.1	99.9	99.9	100.1	99.8	100.0
Cs	1.1	—	31.7	29.8	16.3	0.5	0.7	—	—	—	0.2	0.2
Rb	31.5	1.1	52.7	60	38.3	1.5	5.7	—	—	2.4	17.9	5.6
Sr	165	66	986	1082	1878	153	174	146	153	106	151	52
Ba	341	11	1113	1183	1464	69	20	12	12	23	94	34
Y	23.5	16.8	41.8	44.7	39.9	30.2	6.6	18	18.4	33.8	19.1	30.7
Zr	207.5	42.6	659.1	687.9	627.7	127.3	6.5	41.3	41.9	80.3	82	71.8
Hf	5.3	1.2	14.5	15.9	13.2	2.8	—	1.1	1.5	2.4	3	2
Nb	50.5	0.8	162.1	172.7	155.7	9.2	—	0.7	0.6	1.2	2	1.2
Ta	2.8	—	9.2	9.7	9.3	0.2	—	—	—	—	—	—
Sc	35	35	20	21	19	43	28	38	38	38	3	39
V	234	205	215	224	195	264	97	225	238	304	—	291
Ni	158	92	87	94	95	47	141	60	56	73	28	73
Cu	84	66	24	27	25	77	30	5	5	81	1	53
Zn	74	27	138	177	134	62	12	21	21	90	1	68
Mo	0.4	—	3.1	1.9	4.6	0.7	—	—	—	1	0.2	0
W	—	—	—	—	1	—	—	—	—	—	—	—
Cd	—	—	—	—	0.2	—	—	—	—	0.2	—	—
Sn	2	—	3	2	3	1	2	1	—	—	—	—
As	—	—	2	2	1	1	—	—	—	1	—	1
Tl	0.1	0.1	0.2	0.2	0.1	0.1	0.2	0.1	0.2	0.2	0.2	0.2
Bi	—	—	—	—	—	—	—	—	—	—	—	—
Pb	—	—	7	6	7	—	—		—	—	—	—
Th	4.7	0.1	16.4	15.9	16.1	0.6	—	—	0.2	0.1	1.9	—
U	0.9	0.1	3.1	2.6	4.3	0.4	—	—	—	—	0.5	—
La	44.3	2.1	159.8	167.6	152.8	10.5	1.2	2.3	2.6	3.6	5.6	3.7
Ce	77.6	4.7	272.7	288.9	263.6	21.6	1.6	5.3	5.6	8.4	13.2	8.5
Pr	9.97	0.78	33.17	35.14	32.16	3.17	0.28	0.89	0.95	1.53	1.93	1.53
Nd	42.3	4.5	128.8	138.4	122.5	16.4	1.7	4.8	5.2	9.2	8.4	8.7
Sm	7.2	1.7	20.7	21.9	20.1	4.3	0.5	1.5	1.8	3.2	1.7	2.8
Eu	2.44	0.65	6.5	7.19	5.87	1.55	0.37	0.73	0.79	1.33	0.37	1.2
Gd	6.48	2.42	15.1	14.88	13.51	4.97	1.05	2.59	2.91	4.55	2.61	4.41
Tb	0.97	0.41	1.95	2.22	1.9	0.85	0.16	0.49	0.47	0.86	0.38	0.72
Dy	4.63	2.26	8.65	9.58	8.76	4.95	1.22	2.71	2.84	4.64	2.46	4.55
Ho	0.9	0.61	1.48	1.58	1.39	1.14	0.27	0.71	0.72	1.1	0.63	1.15
Er	2.15	1.79	3.44	3.49	3.34	3.01	0.71	1.83	1.96	3.37	1.98	3.17
Tm	0.28	0.27	0.56	0.49	0.49	0.47	0.12	0.28	0.31	0.61	0.33	0.5
Yb	1.84	1.77	3.17	3.19	2.79	3.23	0.58	1.98	1.89	3.36	2.23	3.06
Lu	0.27	0.27	0.39	0.41	0.43	0.39	0.11	0.28	0.31	0.53	0.37	0.52

Note: Analysis at ACME Analytical Laboratories in Vancouver, British Columbia. Grid coordinates are North American datum (NAD) 83, UTM Zone 8. salts.

JEN01-23-12	JEN01-23-12R	JEN01-26-5a	JEN01-27-6	JEN01-32-1b	MMI01-15-4	MMI01-23-19	YME01-31-7c					
Volcani-clastic	Volcani-clastic	Gabbro	Volcani-clastic	Basalt	Augite-phyric tuff	Basalt	Trachyte	ACME Analytical Laboratories				
Mafic volcanic	Mafic volcanic	Mafic intrusive	Mafic volcanic	Carbonate	carbonate	mafic volcanic	carbonate		CANMET			
IAT	IAT	IAT	IAT	OIB	OIB	E-MORB	OIB	Detection limit	SY4 standard	SY4 ACME	% accuracy	% precision
645419	645419	665924	644156	646677	641793	643810	637065					
6560010	6560010	6551936	6567988	6568948	6566487	6561084	6550442					
48.2	48.0	48.5	53.3	38.9	45.4	46.5	70.5	0.04	49.9	49.84	0.1	0.5
1.33	1.32	0.87	1.09	2.59	3.12	0.70	0.93	0.01	0.29	0.3	3.4	1
15.4	15.3	15.7	14.8	9.5	11.4	17.3	12.4	0.03	20.69	20.93	1.2	0.7
10.5	10.5	9.5	9.9	9.8	12.0	11.0	4.8	0.04	6.21	6.24	0.5	0.4
0.14	0.14	0.14	0.14	0.17	0.14	0.16	0.04	0.01	0.11	0.1	9.1	0
6.6	6.6	8.0	6.6	7.5	9.6	8.7	1.0	0.01	0.54	0.51	5.6	0.1
11.4	11.4	10.1	7.2	16.5	11.4	5.5	1.0	0.01	8.05	8.22	2.1	0.2
2.2	2.2	3.2	4.5	1.7	2.4	2.2	6.1	0.01	7.1	6.79	4.4	0.9
0.3	0.3	0.1	0.5	2.2	1.1	2.3	0.5	0.02	1.66	1.58	4.8	51.5
0.08	0.13	0.05	0.12	0.38	0.49	0.09	0.09	0.01	0.13	0.07	46.2	23.8
0.019	0.018	0.029	0.008	0.052	0.055	0.017	<0.001	0.001	—	<0.001	—	2.7
3.9	4.2	3.8	1.8	10	2.5	5	2.2	0.1	4.56	5	9.6	10.6
0.04	0.05	0.08	0.03	2.48	0.05	0.02	0.11	0.01	—	1.1	—	31.1
0.11	0.07	<0.01	0.03	<0.01	0.01	<0.01	0.18	0.01	—	0.03	—	44.4
100.1	100.0	99.9	100.0	99.5	99.7	99.5	99.9					
0.8	0.9	—	0.1	3.4	1.1	1.6	0.5	0.1	1.5	1.6	6.7	11.8
8.1	7.7	1.1	7.1	52.6	25.5	38.9	14.8	0.5	55	56.6	2.9	5.1
85	86	101	146	445	295	97	516	0.5	1191	1253	5.2	2.9
26	24	24	735	2792	274	1042	2401	5	340	335	1.5	4
29.9	30.7	20	26.1	21.5	25.4	14.7	80.9	0.1	119	132.1	11	2.4
67.4	66.9	37.2	63.5	176.5	217.9	22.4	756	0.5	517	521.7	0.9	1.1
1.8	2	1.3	1.7	4.4	5	0.5	16.5	0.5	10.6	9.7	8.5	20.7
1.2	1.2	—	0.9	38.5	54.7	3.7	182	0.5	13	12.7	2.3	7.7
—	—	—	—	2	2.9	—	9.5	0.1	0.9	0.3	66.7	—
39	38	41	37	33	38	37	6	1	1.1	1	9.1	1.3
301	306	259	293	264	305	217	26	5	8	5	37.5	3.6
62	74	92	102	145	137	156	—	0.1	9	22	144.4	12.3
61	57	70	14	94	77	136	5	0.1	7	3	57.1	3.4
67	62	55	25	59	71	57	38	1	93	49	47.3	3.9
0.7	0.6	—	—	0.3	—	—	0.7	0.1	—	0.2	—	15.4
—	—	—	—	—	—	—	5	0.1	—	—	—	—
—	—	—	—	—	—	—	0.7	0.1	—	—	—	—
—	—	—	—	1	3	5	10	1	7.1	8	12.7	—
1	—	—	1	1	0	1	1	1	—	—	—	—
0.4	0.5	0.3	1.1	0.6	0.2	0.2	0.2	0.1	—	0.1	—	44.5
—	—	—	—	—	—	—	—	0.1	—	—	—	—
—	—	—	—	—	—	—	4	0.1	10	2	80	—
0.2	—	0.2	0.2	3.5	4.6	0.3	12.5	0.1	1.4	1.4	0	—
0.4	0.2	—	—	0.6	0.6	—	2.6	0.1	0.8	1	25	66.7
2.9	2.7	2	2.9	36.1	44.2	2.7	127.1	0.5	58	65.6	13.1	9.7
7.6	8.1	5	6.7	64.3	81.7	5.6	210.9	0.5	122	118.8	2.6	6
1.44	1.35	0.79	1.27	8.19	9.97	0.72	23.91	0.02	15	14.75	1.7	6.5
7.7	8.2	4.9	7.6	37	42.9	4	91	0.4	57	59.6	4.6	7.2
2.7	3	1.5	2.7	7	7.6	1.1	15.2	0.1	12.7	12.7	0	14.4
1.16	1.12	0.74	0.89	2.14	2.77	0.42	3.44	0.05	2	2.2	10	5.7
4.14	4.37	2.59	3.62	5.97	6.39	1.73	12.86	0.05	14	15.49	10.6	8.5
0.76	0.72	0.48	0.66	0.86	0.98	0.36	2.18	0.01	2.6	3	15.4	4.8
5.16	4.83	2.93	4	4.36	4.9	1.92	12.67	0.05	18.2	18.58	2.1	5.7
1.09	1.13	0.7	0.94	0.79	0.89	0.46	2.85	0.05	4.3	4.87	13.3	2.5
3.07	3.02	1.94	2.63	1.73	2.11	1.36	7.07	0.05	14.2	14.84	4.5	4.3
0.45	0.49	0.31	0.42	0.25	0.31	0.25	1.17	0.05	2.3	2.4	4.3	9.4
3.32	2.99	2.17	2.73	1.72	1.95	1.57	7.34	0.05	14.8	16.41	10.9	7.6
0.5	0.46	0.33	0.39	0.23	0.27	0.26	1.18	0.01	2.1	2.34	11.4	9.3

BABB, back-arc basin basalts; calc-alk, calc-alkaline; E-MORB, enriched mid-ocean ridge basalts; IAT, island-arc tholeiites; OIB, ocean-island ba-

Table 2. Whole-rock trace and rare-earth element abundances for mafic rocks in Cache Creek terrane.

Sample:	FDE01-2-16	FDE01-10-13n	FDE01-25-7	FDE01-25-7R	FDE02-2-1a	JBL02-29-3	JBL02-30-2	JEN01-4-4c	JEN01-4-4cR	JEN01-4-7a	JEN01-10-2	JEN01-16-4
Lithology:	Gabbro	Basalt	Diabase	Diabase	Basalt	Gabbro	Volcani-clastic	Diabase	Diabase	Gabbro	Basalt	Diabase
Unit:	Mafic intrusive	Mafic volcanic	Mafic intrusive	Mafic intrusive	Yeth Creek	Mafic intrusive	Mafic volcanic	Mafic intrusive	Mafic intrusive	Mafic intrusive	Carbo-nate	Mafic intrusive
Affinity:	IAT	BABB	BABB	BABB	BABB	IAT	Calc-alk	BABB	BABB	BABB	OIB	BABB
Easting:	618327	640806	661782	661782	618964	597862	597060	643556	643556	644201	635494	597158
Northing:	6545612	6547146	6548782	6548782	6533306	6558357	6558407	6552042	6552042	6551980	6543882	6554432
Li	2	7	5	4	7	3	12	16	12	103	26	7
Cs	0.09	4.13	0.05	0.04	0.20	0.14	0.21	3.74	3.69	1.16	0.60	0.73
Rb	3.1	30.9	1.6	1.5	4.0	0.7	3.2	30.0	29.3	13.1	9.2	3.1
Sr	216	93	451	451	236	31	299	78	85	24	428	137
Ba	74	506	52	53	16	37	20	2405	2346	290	264	31
Y	5.5	35.9	34.6	33.9	22.0	4.9	14.4	38.4	39.0	12.6	27.7	29.5
Zr	7.5	73.4	70.0	66.8	63.0	5.7	92.8	85.9	83.7	24.6	183.8	77.2
Hf	0.9	2.6	2.6	2.7	2.6	0.6	3.2	3.7	3.2	1.4	5.9	2.8
Nb	0.02	1.19	2.14	2.06	1.76	0.03	0.81	4.94	5.37	2.47	48.20	2.78
Ta	0.01	0.09	0.16	0.16	0.12	0.00	0.06	0.36	0.37	0.17	3.26	0.22
Mo	0.12	0.65	1.07	0.29	0.58	0.10	0.76	1.24	1.27	0.12	2.13	0.48
Tl	0.02	0.47	0.05	0.03	0.01	0.03	0.04	0.16	0.18	0.10	0.05	0.03
Bi	0.00	0.03	0.04	0.03	—	0.02	0.10	0.01	0.02	0.00	0.05	0.03
Pb	0.3	0.3	0.5	0.3	0.2	0.1	2.9	0.7	0.7	0.3	3.6	0.9
Th	0.02	0.07	0.13	0.13	0.17	0.03	1.82	0.30	0.27	0.17	4.36	0.19
U	—	0.33	0.09	0.07	0.06	0.03	0.68	0.37	0.42	0.03	1.39	0.08
La	0.12	2.41	3.63	3.57	2.63	0.28	9.25	4.02	4.21	1.82	35.33	3.52
Ce	0.49	7.65	11.63	11.30	8.11	0.62	18.55	11.84	11.93	4.46	80.28	11.19
Pr	0.12	1.50	2.20	2.09	1.38	0.15	2.77	1.98	2.01	0.63	9.60	1.94
Nd	0.90	8.45	11.77	11.69	7.35	0.85	12.04	10.71	11.30	3.19	39.47	9.83
Sm	0.45	3.32	3.98	3.84	2.55	0.44	2.89	4.19	4.03	1.16	8.19	3.50
Eu	0.25	1.24	1.35	1.33	0.99	0.20	0.88	1.68	1.53	0.42	2.40	1.22
Gd	0.75	4.80	5.24	5.18	3.60	0.67	2.79	6.25	5.72	1.75	7.29	4.94
Tb	0.15	0.92	1.01	0.96	0.63	0.14	0.40	1.12	1.12	0.34	1.04	0.87
Dy	1.00	5.77	6.66	6.33	4.33	0.97	2.49	7.74	7.17	2.29	5.82	5.48
Ho	0.23	1.35	1.46	1.39	0.91	0.22	0.49	1.67	1.70	0.55	1.09	1.25
Er	0.66	4.17	4.16	3.87	2.64	0.63	1.44	4.97	4.77	1.66	2.93	3.70
Tm	0.10	0.62	0.66	0.63	0.40	0.10	0.25	0.70	0.73	0.23	0.41	0.54
Yb	0.62	3.87	4.10	4.00	2.56	0.57	1.37	4.54	4.93	1.68	2.38	3.47
Lu	0.08	0.59	0.55	0.52	0.38	0.07	0.20	0.62	0.66	0.25	0.35	0.53

Note: Analysis at Memorial University in St. John's, Newfoundland. Grid coordinates are North American datum (NAD) 83, UTM Zone 8. BABB, back-

a porphyritic trachyte plots in the subalkaline field (rhyolite) in the major-element classification of Fig. 5A, but in the alkaline field in the trace-element classification of Fig. 5B. This sample is plagioclase rich and contains centimetre-sized alkali feldspar phenocrysts, which may skew the analyses owing to their high Si and Na contents and very low Mg, Fe, and Ca concentrations.

Oceanic crustal assemblage

Magmatic rocks from the oceanic crustal assemblage can be separated into four components: (*a*) IAT, (*b*) calc-alkaline arc rocks, (*c*) BABB, and (*d*) E-MORB as demonstrated by the Th–Hf–Nb diagram (Fig. 6). Although the BABB of the oceanic crustal assemblage plot in the normal mid-ocean ridge basalt (N-MORB) field (Fig. 6), it will be demonstrated that trace-element concentrations for these rocks are more consistent with a back-arc setting. A majority of samples from the oceanic crustal assemblage are characterized by low Th/Yb and Nb/Yb ratios indicating that they were derived from a depleted mantle source similar to that for N-MORB (see Th/Yb versus Nb/Yb, Fig. 7).

Island-arc tholeiite suite

The island-arc tholeiites of the oceanic crustal assemblage have higher Th/Yb ratios than N-MORB, indicating the involvement of subduction-derived fluids in their genesis, and lower Nb/Yb ratios than N-MORB, indicating that they may be derived from an even more depleted mantle source (Fig. 7). The low heavy rare-earth element (HREE) content and the overall low positive slope on chondrite-normalized rare-earth element (REE) plots (Fig. 8) are consistent with a source that has experienced depletion in incompatible elements during previous melt extraction (e.g., Pearce and Peate 1995; Pearce 1996).

One of the key features of the IATs of the oceanic crustal assemblage is their pronounced negative Nb and Ta anomalies (Fig. 9), which is most commonly interpreted as a characteristic arc signature (e.g., Jenner 1996; Pearce 1996). These negative Nb and Ta anomalies can be created either by (*i*) preferential retention of Nb and Ta within minor Ti-rich phases, such as rutile in the subducting plate at a convergent margin resulting in the depletion of these elements in any slab-derived fluids or melts that rise and trigger par-

JEN01-26-8a	JEN02-8-1	JEN02-8-1R	JEN02-8-3	JEN02-8-8	JEN02-8-10b	JEN02-8-10bR	JEN02-10-10	JEN02-10-11	JEN02-38-1	JEN02-38-1R	MMI01-2-1
Andesite	Basalt	Basalt	Diabase	Basalt	Gabbro	Gabbro	Gabbro	Gabbro	Basalt	Basalt	Diabase
Mafic volcanic	Mafic volcanic	Mafic volcanic	Mafic intrusive	Mafic volcanic	Mafic intrusive	Mafic intrusive	Mafic intrusive	Mafic intrusive	Yeth Creek	Yeth Creek	Mafic intrusive
E-MORB	BABB	BABB	BABB	BABB	IAT	IAT	Calc-alk	BABB	BABB	BABB	BABB
661585	592147	592147	592094	592824	593329	593329	595372	594919	620731	620731	620109
6553774	6564142	6564142	6563995	6563000	6561958	6561958	6560545	6559654	6533149	6533149	6549063
36	2	2	7	4	2	1	6	10	16	8	7
2.21	0.10	0.10	0.40	0.11	0.18	0.19	0.21	0.38	0.10	0.09	0.56
29.8	4.2	4.8	6.8	7.5	6.1	6.6	24.9	1.2	11.5	12.5	10.3
802	78	80	169	123	320	320	266	354	244	267	556
484	8	8	34	23	17	18	1346	37	31	29	722
10.9	40.1	40.3	35.0	33.3	4.5	4.4	20.8	26.2	25.5	25.8	25.2
44.8	116.1	120.8	85.6	96.8	8.7	5.7	130.3	60.1	65.6	59.4	46.2
2.0	4.1	3.8	4.1	3.2	0.7	0.4	4.9	2.3	2.2	2.1	1.9
9.61	3.03	3.12	2.43	2.53	0.16	0.15	8.53	2.22	1.69	1.65	1.73
0.59	0.25	0.23	0.19	0.20	0.01	0.01	0.65	0.16	0.13	0.14	0.13
0.33	1.43	0.83	0.57	0.40	0.45	0.42	0.40	0.39	0.37	0.34	0.46
0.19	0.04	0.04	0.02	0.04	—	0.02	0.14	0.04	0.07	0.07	0.03
0.03	0.03	0.04	0.03	0.03	—	0.02	0.02	0.05	0.04	0.03	0.03
2.0	0.7	0.7	0.5	0.9	0.3	0.3	2.3	0.5	0.5	0.5	1.0
0.85	0.31	0.31	0.20	0.23	0.05	0.03	3.28	0.17	0.17	0.17	0.15
0.37	0.26	0.25	0.08	0.12	0.01	0.04	1.30	0.09	0.19	0.21	0.08
9.21	4.72	4.63	3.77	3.91	0.37	0.42	17.02	2.96	2.83	2.93	3.02
19.85	14.64	14.07	12.07	12.17	0.98	0.99	37.16	8.62	8.23	8.23	8.72
2.59	2.51	2.46	2.09	2.10	0.17	0.21	4.99	1.52	1.51	1.45	1.53
11.11	13.46	13.31	11.71	11.29	0.91	1.06	21.44	7.92	7.63	8.08	8.59
2.43	4.74	4.49	4.02	3.91	0.40	0.44	4.76	2.74	2.67	2.71	2.91
0.79	1.63	1.60	1.44	1.39	0.36	0.37	1.54	1.07	1.02	1.03	1.07
2.34	6.51	6.11	5.30	5.21	0.64	0.65	4.80	3.95	3.99	3.86	3.82
0.36	1.13	1.06	1.00	0.96	0.12	0.12	0.68	0.65	0.65	0.68	0.71
2.21	7.74	7.70	6.54	6.46	0.88	0.92	4.55	4.59	4.87	5.06	4.99
0.42	1.69	1.58	1.44	1.39	0.20	0.20	0.88	0.95	1.01	1.07	1.08
1.14	5.07	4.70	4.09	4.16	0.60	0.61	2.63	2.90	3.14	3.05	2.88
0.16	0.74	0.73	0.62	0.62	0.09	0.12	0.41	0.46	0.50	0.49	0.47
1.02	4.83	4.39	4.14	3.89	0.62	0.67	2.45	2.52	2.92	3.01	3.00
0.14	0.74	0.63	0.58	0.57	0.09	0.09	0.39	0.40	0.46	0.44	0.40

arc basin basalts; calc-alk, calc-alkaline; E-MORB, enriched mid-ocean ridge basalts; IAT, island-arc tholeiites; OIB, ocean-island basalts.

tial melting of the overlying mantle wedge (e.g., Ryerson and Watson 1987; Brenan et al. 1994; Pearce 1996; Rudnick et al. 2000); (*ii*) contamination with continental crust; (*iii*) remelting of hydrous oceanic crust (e.g., amphibolite) within a rift setting and the generation of Nb-depletions due to the stabilization of Ti-bearing (and amphibolite) phases in the restite (e.g., Haase et al. 2005). However, the Th/Nb to La/Sm ratios of the IATs are not consistent with crustal contamination of a N-MORB magma (Fig. 10), and partial melting of hydrous oceanic crust generally produces more silicic (andesitic–dacitic) magmas (e.g., Green and Pearson 1987; Beard and Lofgren 1991; Haase et al. 2005) that have not been described in the oceanic crustal assemblage of the Nakina area. Therefore, an arc origin is the preferred model for this suite of rocks (see "subduction enrichment" in Fig. 10).

Calc-alkaline suite

Calc-alkaline arc rocks from the oceanic crustal assemblage plot along the liquid-fractionation vector, suggesting that these calc-alkaline rocks may have evolved from the more primitive IATs (Fig. 7). The low HREE contents (Fig. 8) suggest that the source of these arc rocks may be even more depleted than a MORB source (e.g., Pearce and Peate 1995). The primary difference in the REE patterns between the IATs and the calc-alkaline rocks is that the calc-alkaline rocks are enriched in light rare-earth elements (LREE; this enrichment in LREE may be a consequence of fractional crystallization and progressive enrichment in incompatible elements. The calc-alkaline rocks also exhibit pronounced negative Nb and Ta anomalies and are relatively enriched in Th, indicating that subduction-derived fluids may have been involved in magma genesis (Fig. 9).

Back-arc basin basalt suite

The BABB of the oceanic crustal assemblage have similar Th/Yb and Nb/Yb ratios (Fig. 7) and REE patterns (Fig. 8) to N-MORB, indicating that they were derived from a depleted mantle source. However, the BABB of the oceanic crustal assemblage is distinguished from N-MORB, as BABB display a slight negative Nb anomaly and enrichment in Th. Such features suggest arc affinity (Fig. 9) and perhaps

Table 2. (*concluded*).

Sample:	MMI01-4-2	MMI01-6-9	MMI01-27-6	MMI01-27-6R	MMI02-10-2-	MMI02-11-3	MMI02-13-7	MMI02-15-7-4	MMI02-21-11	MMI02-28-4	MMI02-31-9
Lithology:	Basalt	Diabase	Tonalite	Tonalite	Gabbro	Quatrz-phyric tuff	Gabbro	Basalt	Basalt	Volcani-clastic	Fspar-phyric dyke
Unit:	Mafic volcanic	Carbonate	Mafic intrusive	Mafic intrusive	Mafic intrusive	—	Mafic intrusive	Mafic volcanic	Carbonate	Carbonate	Carbonate
Affinity:	BABB	OIB	IAT	IAT	BABB	E-MORB	IAT	IAT	OIB	OIB	OIB
Easting:	640350	638450	659068	659068	593404	627000	598260	597129	615533	593765	637600
Northing:	6552200	6561530	6544625	6544625	6558638	6550811	6556848	6558876	6558876	6568414	6568450
Li	11	47	2	2	6	49	18	18	23	30	29
Cs	1.42	0.99	0.16	0.15	0.76	0.86	1.87	0.91	0.46	0.29	6.90
Rb	30.4	37.8	1.1	1.0	6.9	35.7	36.2	41.3	21.1	9.1	78.2
Sr	76	195	49	50	158	417	310	266	814	186	334
Ba	76	2519	31	30	83	1239	56	143	666	336	727
Y	29.9	23.5	9.9	9.9	32.9	26.3	3.0	16.5	21.0	33.0	26.0
Zr	69.2	231.0	17.7	17.4	89.3	55.5	4.6	32.7	120.8	108.2	178.5
Hf	2.6	6.6	0.8	0.8	3.1	2.3	0.5	1.5	4.5	3.4	5.3
Nb	1.70	67.01	1.58	1.25	3.05	12.77	0.03	0.74	56.20	54.26	68.44
Ta	0.12	4.19	0.16	0.13	0.22	0.81	0.01	0.05	3.39	3.46	4.78
Mo	0.29	2.80	0.18	0.12	0.47	0.27	0.15	0.76	0.75	0.60	1.83
Tl	0.24	0.11	0.07	0.03	0.06	0.04	0.39	0.63	0.06	0.11	0.33
Bi	0.04	0.02	0.06	0.03	0.04	0.02	0.06	0.07	0.00	0.07	0.05
Pb	0.6	4.8	1.0	0.6	0.8	3.6	0.2	11.0	1.6	0.8	1.8
Th	0.13	5.38	0.18	0.19	0.26	1.01	0.03	0.26	4.07	4.86	3.79
U	0.16	1.31	0.22	0.20	0.13	0.33	0.06	0.11	0.82	0.84	2.26
La	2.95	43.48	2.20	2.21	4.19	8.38	0.27	5.15	39.41	39.77	44.12
Ce	9.97	92.44	4.99	5.21	13.08	18.15	0.47	7.05	76.45	71.74	93.80
Pr	1.97	11.50	0.81	0.75	2.22	2.35	0.17	1.72	9.24	8.78	12.20
Nd	10.07	43.52	3.51	3.53	11.95	10.15	0.65	8.12	38.06	34.26	51.20
Sm	3.70	8.46	1.12	1.07	4.03	2.73	0.32	2.41	7.57	6.85	10.67
Eu	1.32	2.78	0.35	0.33	1.43	0.90	0.21	0.85	2.73	2.18	3.02
Gd	5.29	7.22	1.34	1.26	5.49	3.52	0.41	2.94	6.67	6.42	9.14
Tb	0.91	0.96	0.23	0.24	0.99	0.66	0.08	0.51	0.90	0.92	1.21
Dy	6.40	5.78	1.75	1.74	6.68	4.85	0.56	3.31	5.12	5.87	6.75
Ho	1.31	0.95	0.35	0.35	1.45	1.07	0.12	0.67	0.90	1.06	1.14
Er	3.78	2.43	1.11	1.09	4.12	3.23	0.39	1.85	2.16	2.88	2.77
Tm	0.58	0.32	0.23	0.21	0.63	0.49	0.11	0.29	0.26	0.42	0.37
Yb	3.49	1.73	1.03	1.08	3.93	3.31	0.30	1.56	1.50	2.05	1.85
Lu	0.50	0.23	0.14	0.15	0.56	0.49	0.04	0.21	0.20	0.28	0.25

a genetic linkage between BABB and both IATs and the calc-alkaline rocks of the oceanic crustal assemblage.

Enriched mid-ocean ridge basalt suite

E-MORB type rocks are a minor component of the oceanic crustal assemblage. They display Th/Yb and Nb/Yb values transitional between N-MORB and OIB (Fig. 7), indicating derivation from a slightly more enriched mantle source than the rest of the oceanic crustal assemblage. E-MORBs display slight LREE enrichment relative to N-MORB, and some are HREE depleted with respect to N-MORB (compare Figs. 8*c*, 8*f*). Significantly, E-MORBs differ from the other oceanic crustal assemblage because they lack a negative Nb–Ta arc signature (see “source enrichment” in Figs. 9, 10).

Yeth Creek formation — back arc basin basalt

Pillow basalts from the Yeth Creek formation are geochemically identical to BABB from the oceanic crustal assemblage of the Cache Creek terrane (Fig. 6). Both display Th/Yb and Nb/Yb ratios (Fig. 7) and REE patterns (Fig. 8) similar to N-MORB, indicating that they were derived from a depleted mantle source. Both also display a slight Nb depletion and Th enrichment, possible indicators of an arc affinity (Fig. 9). Despite strong geochemical similarity between the Yeth Creek formation and the oceanic crustal assemblage, corroborating evidence for their correlation is lacking at present.

Carbonate unit — ocean-island type

Volcanic rocks from the carbonate unit are alkaline within-plate basalts and differentiate as determined by their Th–Hf–Nb contents (Fig. 6). These alkaline volcanic rocks are characterized by high Th/Yb and Nb/Yb ratios (Fig. 7) and a pronounced negative slope in REE due to significant enrichment in LREE (Fig. 8), indicating that they were derived from an enriched mantle source (Fig. 10) similar to that of OIB. Of the incompatible elements, only HREE are not enriched relative to N-MORB (e.g., Yb). HREE are

MMI02-33–10	MMI02-34–1	MMI02-34–1R	MMI02-34-2-3	OP2–01i	YME01-23–2	YME01-23–2R					
andesite	basalt	basalt	volcani-clastic	volcani-clastic	basalt	basalt					
mafic volcanic	Yeth Creek	Yeth Creek	mafic volcanic	mafic volcanic	carbonate	carbonate					
E-MORB	BABB	BABB	IAT	IAT	OIB	OIB					
602970	618929	618929	621390	597200	630949	630949	Memorial University				
6565290	6533263	6533263	6543778	6558236	6560606	6560606	Detection Limit	MRG-1 Standard	MRG-1 MUN	% Accuracy	% Precision
24	17	13	14	21	73	87	1.872	3.71	2.58	30.5	31.7
0.11	0.14	0.14	0.46	0.92	2.79	2.78	0.029	0.6	0.62	3.3	6.2
8.2	10.3	11.2	16.4	19.0	39.5	39.3	0.058	7.65	6.57	14.1	5.7
190	131	139	144	237	167	162	1.36	274	257.93	5.9	3.8
205	165	158	104	84	264	275	2.81	47.5	63.01	32.7	4.2
6.3	36.9	36.1	23.5	19.7	18.9	20.2	0.01	11.6	10.16	12.4	2.2
19.8	104.8	102.8	44.0	66.4	44.0	51.7	0.238	93.7	95.36	1.8	10.3
1.2	3.9	3.6	1.9	2.5	1.7	2.2	0.018	3.76	4.66	23.9	16.6
1.90	4.12	4.19	0.97	1.51	11.78	11.55	0.003	22.3	22.96	3	6.2
0.14	0.33	0.32	0.08	0.13	0.78	0.71	0.003	0.83	1.07	28.9	6.7
0.47	2.30	2.41	0.36	2.25	0.26	0.41	0.131	1.26	1.13	10.3	34.1
0.06	0.07	0.08	0.29	0.30	0.12	0.06	0.031	0.05	0.06	20	30.5
0.01	0.04	0.04	0.05	0.11	0.05	0.02	0.034	0.13	0.09	30.8	45.3
1.8	0.4	0.9	2.4	4.0	1.3	1.7	0.687	5.2	4.88	6.2	28.3
0.26	0.32	0.30	0.13	0.17	0.72	0.68	0.004	0.78	0.89	14.1	9.5
0.29	0.15	0.15	0.30	0.13	0.35	0.30	0.033	0.25	0.28	12	22.4
2.03	4.85	4.83	2.97	3.70	11.23	10.92	0.021	9.07	9.32	2.8	3.6
4.99	14.69	14.32	7.05	9.03	26.29	28.79	0.024	26.2	25.38	3.1	3.2
0.78	2.55	2.45	1.33	1.83	3.87	3.97	0.015	3.79	3.97	7.1	6.2
3.91	12.92	12.94	6.98	9.31	18.79	18.69	0.043	18.3	19.09	4.3	3.7
1.10	4.52	4.33	2.55	3.09	5.06	4.80	0.041	4.51	4.58	1.6	4.8
0.50	1.66	1.58	0.92	1.22	1.61	1.58	0.032	1.46	1.44	1.7	3.8
1.26	6.09	5.81	3.47	3.95	4.84	4.69	0.031	4.11	3.96	3.6	4.5
0.19	1.05	1.02	0.61	0.66	0.75	0.70	0.008	0.55	0.56	1.8	3.9
1.22	7.16	7.00	3.97	4.38	4.59	4.21	0.022	3.01	3.03	0.7	4.2
0.25	1.50	1.49	0.87	0.87	0.83	0.73	0.007	0.51	0.53	3.9	4.3
0.69	4.63	4.33	2.64	2.47	1.99	1.97	0.015	1.21	1.26	4.1	4.2
0.10	0.71	0.66	0.40	0.39	0.27	0.24	0.011	0.15	0.17	13.3	8.7
0.64	4.14	4.00	2.24	2.23	1.28	1.23	0.009	0.81	0.95	17.3	5.4
0.09	0.63	0.60	0.34	0.29	0.12	0.14	0.017	0.11	0.12	9.1	7.4

compatible with garnet (e.g., Pearce 1996), and this signature may reflect derivation from a deeper garnet lherzolite source as opposed to a shallower mantle source region for N-MORB. Volcanic rocks of the carbonate unit do not exhibit an arc affinity (Figs. 9, 10).

Petrogenetic interpretations

Lithogeochemical data from the Nakina area indicate that the northern Cache Creek terrane is dominated by two different petrogenetic components: alkaline volcanic rocks of within-plate affinity and subalkaline intrusive and extrusive rocks mostly of arc affinity. The alkaline volcanic rocks interbedded with Carboniferous carbonate were derived from an enriched mantle source and are compositionally identical to OIB. These volcanic rocks were, therefore, probably erupted in a within-plate oceanic setting supporting earlier suggestions that oceanic seamounts and (or) plateaus were the elevated oceanic basement on which the shallow-water carbonate platforms of the Cache Creek terrane were deposited (Monger 1975). Biochronological data constrain the age of the oceanic seamounts to older than the Permo-Carboniferous carbonates that stratigraphically overlie the alkaline volcanic rocks (Monger 1975; Mihalynuk et al. 2002, 2003*a*). Hence, these carbonate rocks were probably deposited on volcanic seamounts in a separate Tethyan faunal province and subsequently transported into the North American realm on the oceanic crust. The alkaline volcanic rocks that underlie and are locally interbedded with carbonate strata are volumetrically minor; and it appears that the majority of the volcanic basement to the carbonate atolls was either underplated at greater depth in the subduction complex or subducted completely.

The subalkaline intrusive and extrusive rocks of the oceanic crustal assemblage consist of IATs and BABB- and E-MORB-type volcanic rocks. The IATs, calc-alkaline arc rocks, and BABB were all derived from a depleted mantle source similar to N-MORB. The IATs and calc-alkaline arc rocks display depleted Nb and enriched Th contents and are

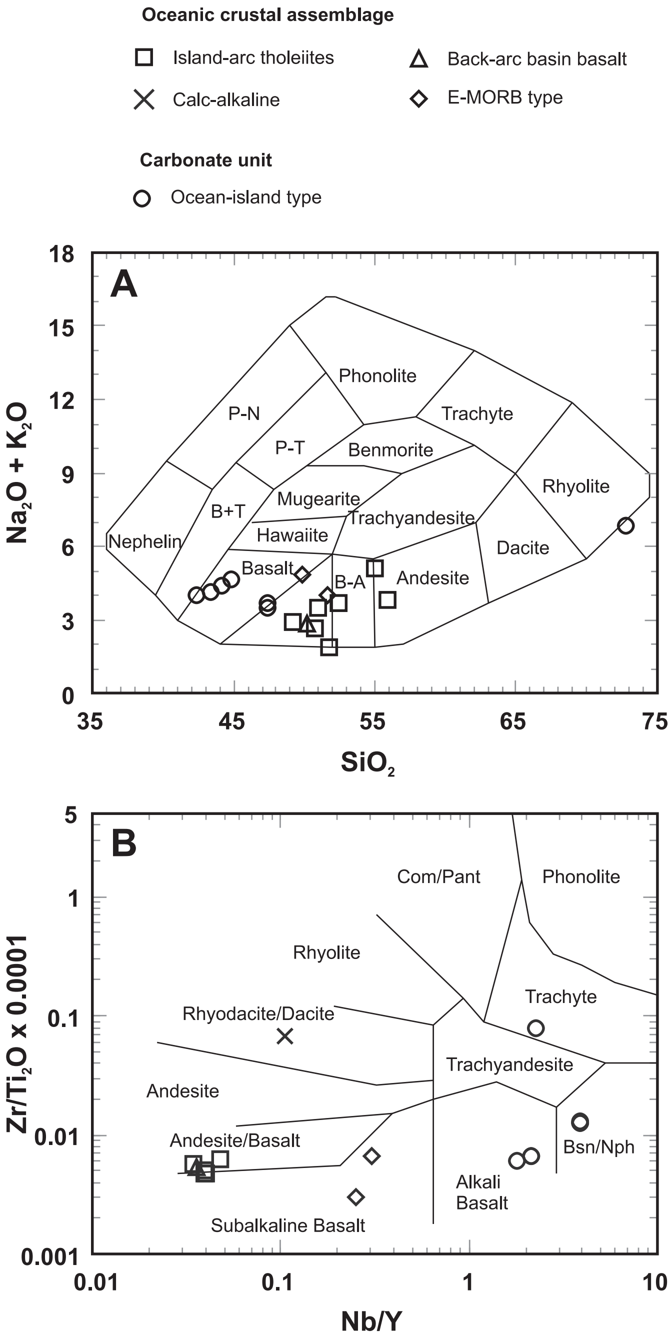

Fig. 5. Nakina area lithogeochemical data plotted on rock classification diagrams. Volcanic rocks from the carbonate assemblage are alkaline and range from alkali basalts and basanites to trachytes, whereas rocks from the oceanic crustal assemblage are subalkaline and dominantly basaltic and basaltic–andesitic in composition. (A) Na_2O+K_2O versus SiO_2 total alkalis versus silica (TAS) diagram (from Cox et al. 1979). B-A, basaltic andesite; B+T, basanite + tephrite; P–N, phonolite–nephelinite; P–T, phonolite–tephrite. (B) Immobile trace-element abundances are also used for rock classification (from Winchester and Floyd 1977), particularly in altered volcanic rocks where elemental mobility is suspected. Bsn/Nph, basanite–nephelinite; Com/Pant, comendite–pantellerite.

interpreted to have formed in a subduction zone setting. Isotopic age dates from some of these rocks are Middle to Late Permian (Devine 2002; Mihalynuk et al. 2003*a*), and those from south of the Nakina area range into the earliest Triassic (Childe et al. 1998). Basalts from the oceanic crustal assemblage that are interpreted to have originated in a back-arc setting are compositionally similar to N-MORB but display a weak subduction zone signature. E-MORB type volcanic rocks are a minor component of the oceanic crustal assemblage and do not display a subduction zone signature.

Pillow basalts from the Yeth Creek formation are compositionally identical to BABB of the oceanic crustal assemblage and, hence, it is possible that the ‘‘ophiolitic’’ belt of the northern Cache Creek terrane may represent basement to Upper Triassic – Middle Jurassic arc-marginal sedimentary rocks of the Whitehorse Trough. It is important to note, however, that the ages of the BABB of the oceanic crustal assemblage and Yeth Creek formation have not yet been independently verified.

Coexistence of IATs, calc-alkaline arc rocks, and BABB- and E-MORB-type volcanic rocks within the oceanic crustal assemblage constrains the tectonic setting of the Cache Creek complex. The IATs and calc-alkaline arc rocks record a period of arc magmatism during Middle to Late Permian time. Given that back-arc basins generally produce magmas that are transitional between MORB and volcanic arc rocks (e.g., Pearce 1996), it is possible that all of the compositions represented in the oceanic crustal assemblage could have been produced in an arc to back-arc setting during the Middle to Late Permian. Alternatively, it is possible that the IATs and calc-alkaline arc rocks represent the early products of arc magmatism that intruded into and erupted onto older back-arc oceanic crust (as discussed in English and Johnston 2005). However, at present, there are insufficient biochronological and faunal data to test this hypothesis. It is also possible that E-MORB of the oceanic crustal assemblage may represent slivers of oceanic crust that were sliced off the subducting slab and incorporated into the Cache Creek subduction complex; therefore, it is possible that these rocks have a closer genetic association with the within-plate volcanic rocks than with the arc rocks of the oceanic crustal assemblage.

Comparisons with other data from the northern Cache Creek terrane

Volcanic rocks are also associated with Tethyan carbonate in other parts of the northern Cache Creek terrane. In the Hall Lake area (Fig. 1), massive basalt, basaltic breccia, and trachyandesitic tuff are in stratigraphic contact with fossiliferous, massive carbonate rocks that contain Permian fusulinids (Monger 1975; Mihalynuk and Cordey 1997). These volcanic rocks are compositionally identical to alkaline volcanic rocks from the carbonate unit in the Nakina area (Fig. 11).

Volcanic rocks in the French Range area (Fig. 1) are dominated by basaltic to trachyandesitic tuff, massive fine-grained flows and pillowed flows that can be up to a few hundred metres thick (Mihalynuk and Cordey 1997); these volcanic rocks are also associated with Tethyan carbonate rocks. A quartz-phyric rhyodacite in the French Range has

Fig. 6. The Th–Hf–Nb discrimination diagram can be used to discriminate between mafic volcanic rocks produced in different settings because these elements are less susceptible to mobility during low-grade metamorphism and their concentrations, therefore, relate to original magmatic processes (Wood 1980). Arc magmas display depletion in high field-strength elements (HFSE; especially Nb and Ta) coupled with enrichment in low field-strength element (LFSE; e.g., Th) relative to other HFSE (e.g., Wood 1980). Calc-alkaline rocks are the common products of arc magmatism and tend to be characterized by a greater enrichment in Th relative to Hf (Hf/Th < 3); they can, therefore, be distinguished from more primitive island-arc tholeiites (IAT) using a Th–Hf–Nb diagram (Wood 1980). Non-arc rocks can also be classified using this diagram because normal mid-ocean ridge basalts (N-MORB) have low Nb contents and high Hf/Nb ratios, whereas ocean-island basalts (OIB) have higher Nb contents and lower Hf/Nb ratios. Basaltic rocks from marginal basins (e.g., back-arc basin basalts (BABB)) can plot within the N-MORB (Pearce 1996), and hence discrimination between these two tectonic environments may be difficult. The fields on the diagram can be defined as (A) N-MORB, (B) enriched mid-ocean ridge basalts (E-MORB) and tholeiitic within-plate basalts and differentiates, (C) alkaline within-plate basalts and differentiates, and (D) destructive plate-margin basalts and differentiates. Magmatic rocks from the oceanic crustal assemblage can be separated into four components: calc-alkaline arc rocks, IAT, BABB/N-MORB, and E-MORB. Pillow basalts from the Yeth Creek assemblage are geochemically identical to BABB/N-MORB from the oceanic crustal assemblage of the Cache Creek terrane. Volcanic rocks from the carbonate unit are classified as alkaline within-plate basalts and differentiates. Only mafic samples are plotted on this diagram.

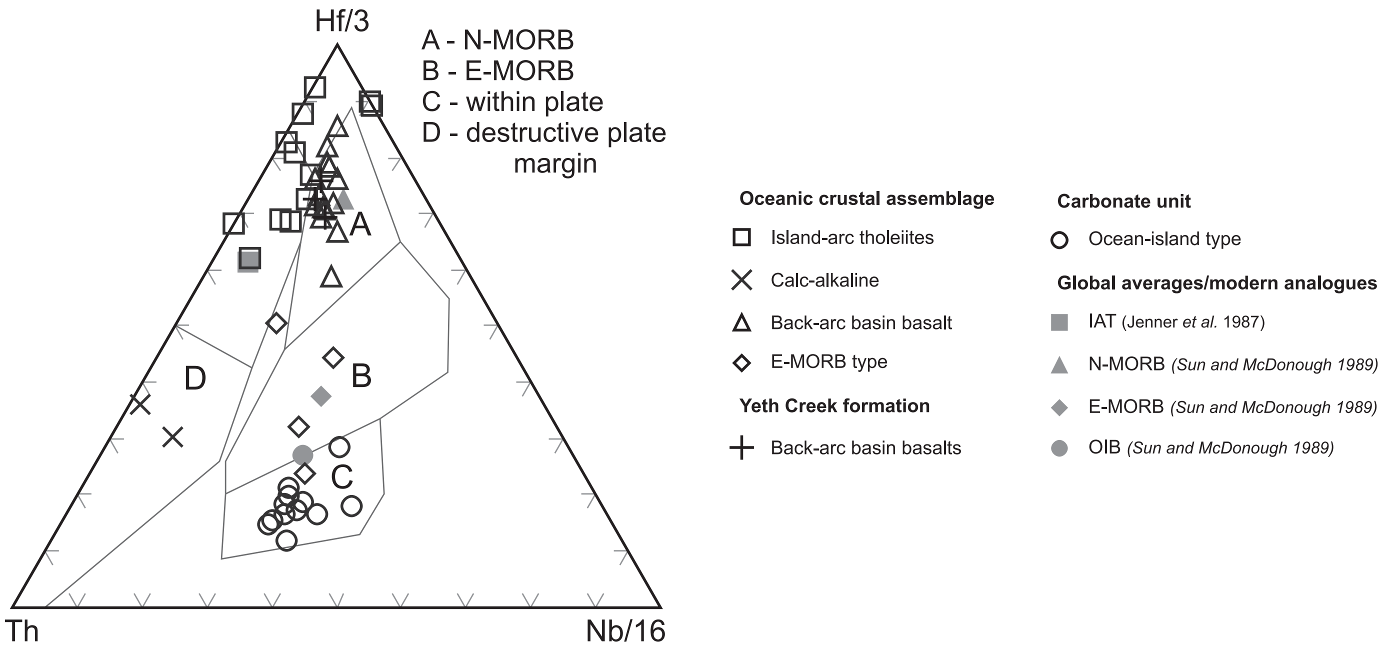

been dated at ~263 Ma using U/Pb methods (Mihalynuk et al. 2004*a*). This date is consistent with the age of stratigraphically overlying Middle Permian carbonate rocks (Monger 1969). Hence, these volcanic rocks are younger than the alkaline volcanic rocks of the carbonate unit in the Nakina area and are similar in age to slightly older than the subalkaline arc rocks of the oceanic crust assemblage. However, the French Range volcanic rocks are E-MORB and tholeiitic within-plate basalts derived from an incompatible element-enriched mantle source, but they are not as enriched as other carbonate-associated volcanic rocks in the Cache Creek terrane and do not contain a subduction zone signature (Fig. 11). Given the signature of the French Range volcanic rocks and their association with Tethyan carbonate rocks, it is proposed that these volcanic rocks also represent the remnants of oceanic islands that were scraped off the downgoing slab and accreted at a convergent margin. The French Range successions are unique in the northern Cache Creek terrane, as they have been metamorphosed to blueschist grade (Monger 1969; Mihalynuk and Cordey 1997; Mihalynuk et al. 2004*a*). Blueschist is exposed over an area of <100 km^2, centered ~40 km west of Dease Lake (Fig. 1)

The Kutcho assemblage lies to the southwest of the Nahlin Fault in the Dease Lake area (Fig. 1), where it is interpreted as basement to Upper Triassic and Lower Jurassic sedimentary rocks of the Whitehorse Trough (Thorstad and Gabrielse 1986; Gabrielse 1998). The dominantly volcanic Kutcho assemblage contains compositionally bimodal, interbedded basalt and rhyodacite to rhyolite, with minor sedimentary intervals (Childe and Thompson 1997; Childe et al. 1998). Fine-grained rhyolitic tuffs from the upper part of the succession have been dated at 246 ± 6 and 242 ± 1 Ma (Childe and Thompson (1997); Early to Lower Middle Triassic, Walker and Geissman (2009)). The Kutcho assemblage volcanic rocks are tholeiitic, and their depleted high field-strength element and flat to LREE-depleted REE patterns suggest that they were formed in an intraoceanic arc environment (Barrett et al. 1996; Childe et al. 1998). Felsic tuff of the Kutcho assemblage is compositionally similar to Eocene tholeiitic rhyolites that occur in the forearc of the

Fig. 7. The Th/Yb versus Nb/Yb plot can be used to assess the level of depletion in the mantle source (e.g., Pearce 1982; Pearce et al. 1995; Metcalf et al. 2000). Each ratio consists of the concentration of a more incompatible element divided by the concentration of a less incompatible element such that previous melt extraction from the mantle source will result in a decrease in both ratios. The normal mid-ocean ridge basalt field (N-MORB) is derived from a depleted mantle source that experienced depletion in incompatible elements during previous melt extraction, whereas ocean-island basalts (OIB) is derived from an enriched mantle source. The source depletion vector indicates increasing levels of mantle source depletion produced by prior melt extraction. The presence of subduction-derived fluid prior to magma genesis increases the Th/Yb ratio, but not the Nb/Yb ratio, in the resulting melt. Liquid- and cumulate-fractionation vectors parallel the source depletion vector. The majority of samples from the oceanic crustal assemblage and the Yeth Creek assemblage are characterized by low Th/Yb and Nb/Yb ratios, indicating that they were derived from a depleted mantle source similar to that for N-MORBs. The island-arc tholeiites and calc-alkaline arc rocks of the oceanic crustal assemblage have higher Th/Yb ratios, indicating the importance of subduction-derived fluids in their genesis. Calc-alkaline arc rocks from the oceanic crustal assemblage plot along the liquid-fractionation vector, suggesting that these calc-alkaline rocks may have evolved from the more primitive island-arc tholeiites. Volcanic rocks from the carbonate unit are characterized by high Th/Yb and Nb/Yb ratios, indicating that they were derived from an enriched mantle source similar to that for OIBs. Only mafic samples are plotted on this diagram.

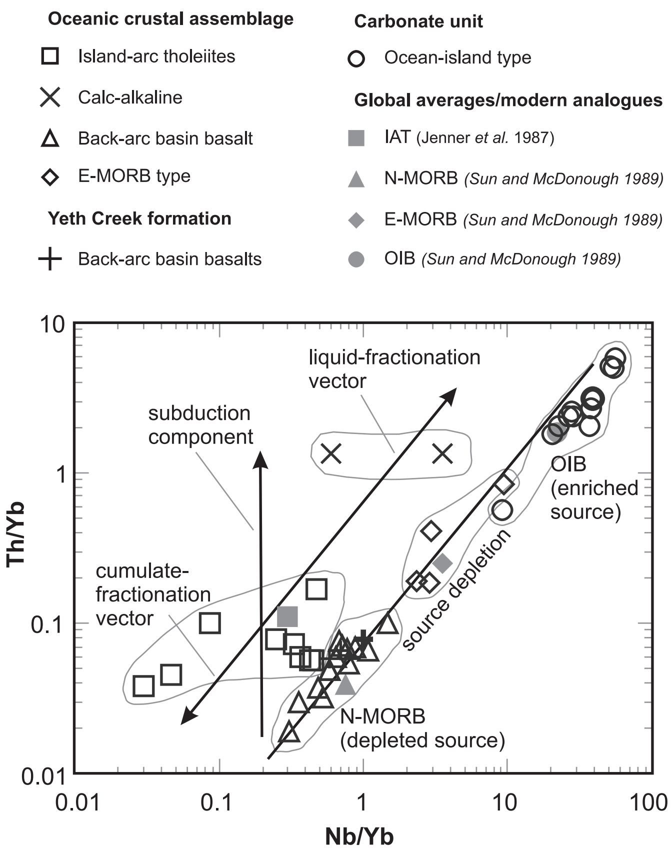

Tonga magmatic arc, and likely erupted in a similar nascent arc setting (Barrett et al. 1996).

English and Johnston (2005) proposed that the island-arc tholeiites and calc-alkaline arc rocks of the oceanic crustal assemblage of the northern Cache Creek terrane can be correlated with the coeval to slightly younger, geochemically similar Kutcho assemblage (Fig. 11). This correlation was based on three lines of evidence: (1) position along the western margin of the Cache Creek terrane (Fig. 1), (2) primitive oceanic island-arc tholeiitic chemistries (Fig. 11), and (3) Middle Permian to Middle Triassic ages. Indeed, a quartz-rich clastic unit that unconformably overlies the oceanic crustal assemblage of the Cache Creek terrane in the Nakina area is characterized by a predominance of Early Triassic detrital ages for which the Kutcho assemblage appears to be the only viable source (Mihalynuk et al. 2003*b*). Together, the island-arc tholeiites and calc-alkaline arc rocks of the oceanic crustal assemblage of the Cache Creek terrane and the Kutcho assemblage may represent incipient arc magmatism during the Late Permian and Middle Triassic. This nascent arc assemblage may have subsequently occupied a fore-arc position adjacent to the developing Cache Creek subduction complex during Late Triassic and Early Jurassic arc magmatism in the Stikine terrane (see detailed discussion in English and Johnston 2005). Alternatively, the Kutcho – Cache Creek assemblage may represent an entirely separate intraoceanic arc that was amalgamated with the Stikine arc during growth of the Cache Creek subduction complex.

Accretionary processes in the northern Canadian Cordillera

The subalkaline oceanic crustal assemblage of the northern Cache Creek terrane can be interpreted as a section of supra-subduction zone oceanic lithosphere that was emplaced during arc–arc or arc–continent collision in the Middle Jurassic. On the other hand, the alkaline volcanic rocks of the Nakina area constitute a volumetrically minor component within Carboniferous–Triassic carbonate successions that bear Early Permian Tethyan fauna exotic to the rest of North America. These volcanic horizons tend to be associated with the oldest (Mississippian) carbonate strata, suggesting that the carbonate successions were deposited atop elevated volcanic basement within the ocean basin. These carbonate and volcanic rocks are, therefore, interpreted to represent the remnants of oceanic seamounts that were “sliced off” and incorporated into a subduction complex at a convergent margin along with other hemipelagic and siliciclastic sedimentary rocks, as previously proposed by Monger (1975). The absence of voluminous ocean-island basalt suggests that the volcanic basement to the carbonate atolls was either underplated at greater depth in the subduction complex or subducted completely. Hence, it is apparent that accretionary processes work effectively only for low-density materials composing the upper portion of the subducting oceanic plate, supporting similar conclusions drawn from accretionary belts in Japan (Isozaki et al. 1990). A greater volume of within-plate volcanic rocks is preserved in the French Range portion of the Cache Creek terrane with volcanic accumulations reaching a few hundred metres in thick-

Fig. 8. Chondrite-normalized rare-earth element (REE) plots for samples from the Nakina area. Normalizing values are from Taylor and McLennan (1985).

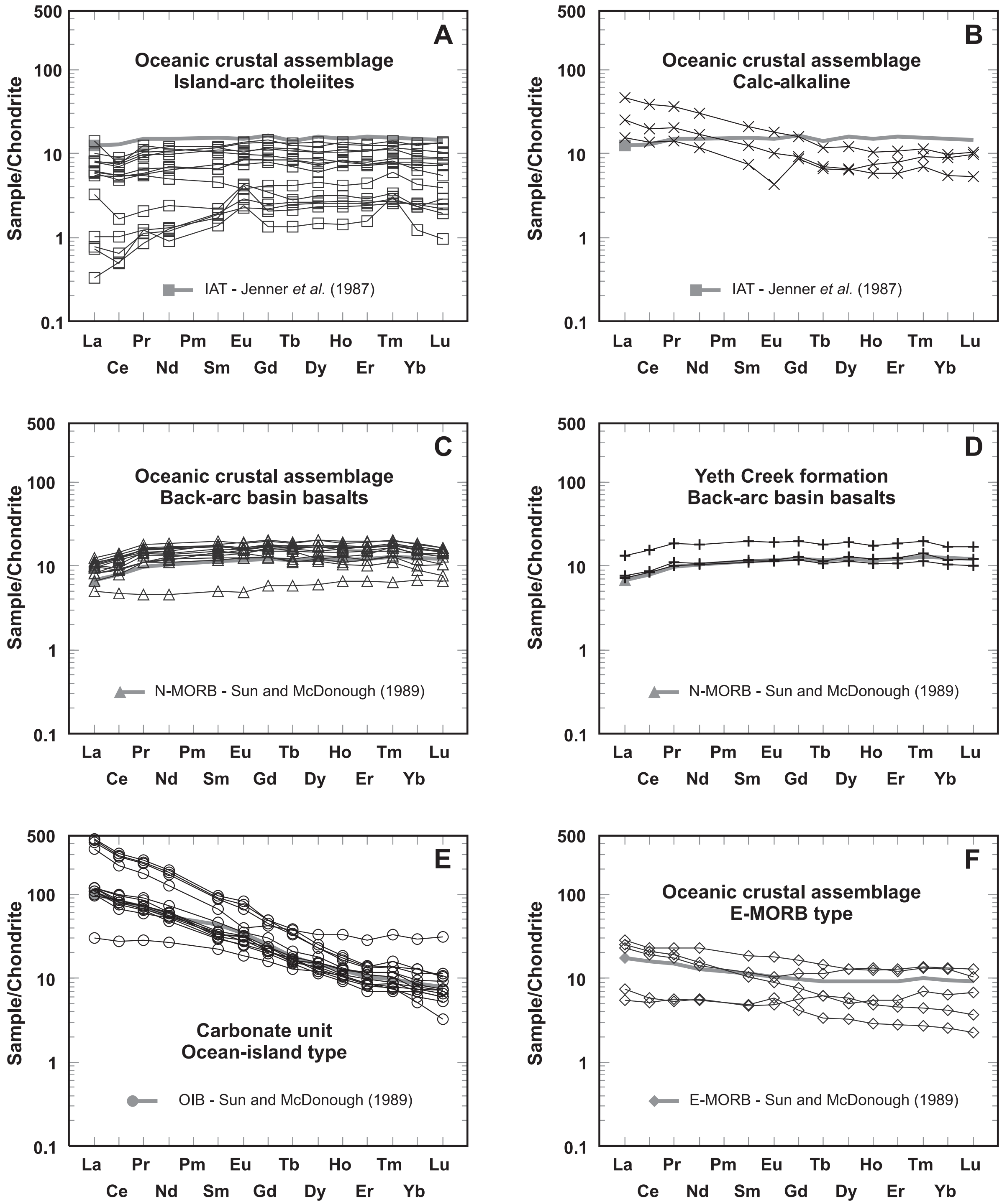

Fig. 9. Trace element spider diagrams for samples from the Nakina area. Data are normalized to normal mid-ocean ridge field (N-MORB) using the values from Sun and McDonough (1989).

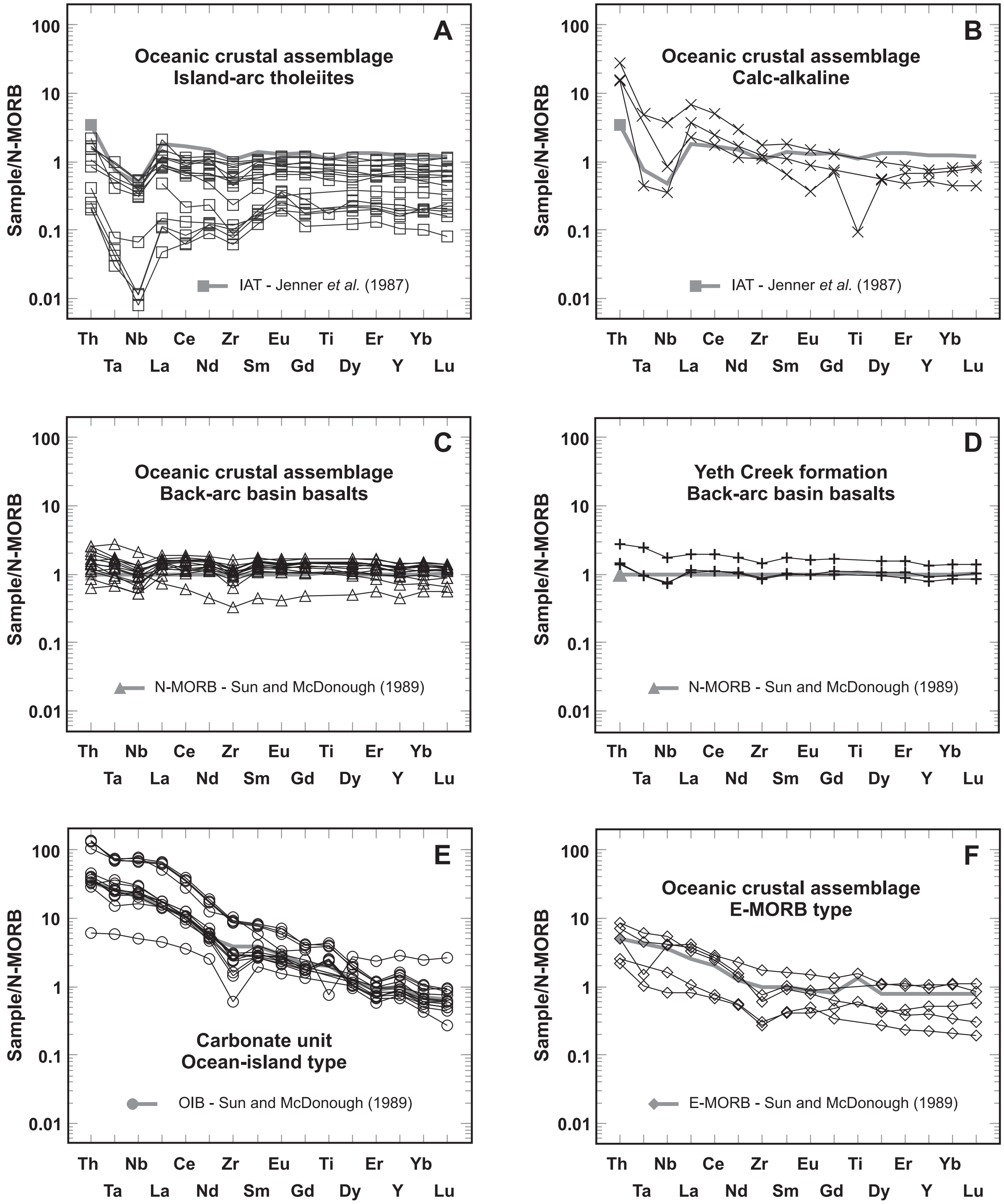

Fig. 10. A Th/Nb versus La/Sm plot can be used to differentiate between within-plate enrichment, subduction zone enrichment, and crustal contamination (modified from Piercey et al. 2002). The island-arc tholeiites (IATs) of the oceanic crustal assemblage plot along a subduction enrichment trend, whereas the enriched mid-ocean ridge basalts (E-MORBs) and ocean-island basalts (OIBs) plot along a within-plate enrichment trend.

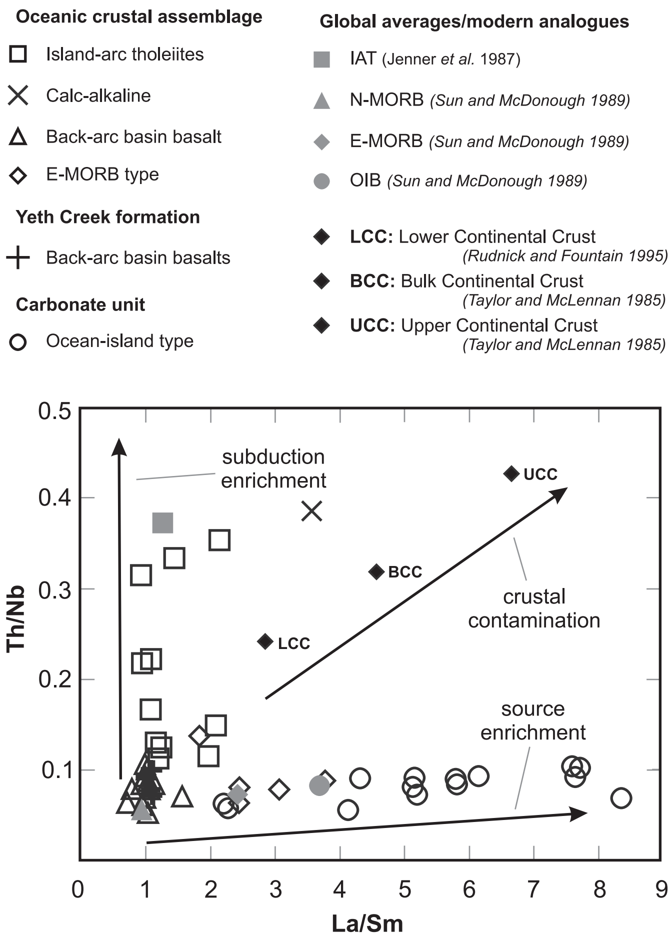

ness (Mihalynuk and Cordey 1997). These French Range volcanic rocks are blueschist grade, contrasting with prehnite–pumpellyite to pumpellyite–actinolite facies metamorphism in the Nakina area. Hence, it is possible that the volumetric proportion of accreted oceanic volcanic rocks may increase with an increase in depth, as has been proposed for accretionary complexes in Japan (Isozaki et al. 1990), indicating that underplating may be a more important process than offscraping for the accretion of oceanic materials to the upper plate.

Acknowledgements

This research was funded by the British Columbia Ministry of Energy and Mines and the Geological Survey of Canada, by a University of Victoria Fellowship and two Geological Society of America Student Research Grants to J.E., and by a Natural Sciences and Engineering Research Council of Canada (NSERC) Discovery Grant to S.T.J. Thanks to the rest of the crew who worked in the Cache Creek terrane as part of this project: Fabrice Cordey, Fionnuala Devine, Yann Merran, Kyle Larson, Adam Bath, Jacqueline Blackwell, and Oliver Roenitz; and also to Norm Graham at Discovery Helicopters for logistical assistance. This manuscript has benefited from discussions with and comments by Dante Canil, Kathy Gillis, Brendan Murphy, Craig Hart, Jim Monger, Paul Schiarizza, Nick Massey, Chris Ash, Graham Nixon, and Roberta Rudnick. This manuscript has also been improved by constructive reviews from Cees van Staal, Steve Piercey, and Maurice Colpron.

References

Aitken, J.D. 1959. Atlin map-area, British Columbia. Geological Survey of Canada, Memoir 307.

Ash, C.H. 1994. Origin and tectonic setting of ophiolitic ultramafic and related rocks in the Atlin area, British Columbia (NTS 104N). British Columbia Ministry of Energy, Mines and Petroleum Resources, Bulletin 94.

Barrett, T.J., Thompson, J.F.H., and Sherlock, R.L. 1996. Stratigraphic, lithogeochemical and tectonic setting of the Kutcho Creek massive sulphide deposit, northern British Columbia. Exploration and Mining Geology, **5**: 309–338.

Bath, A. 2003. Atlin TGI, Part IV: Middle Jurassic granitic plutons within the Cache Creek terrane and their aureoles: Implications for terrane emplacement and deformation. *In* Geological fieldwork 2002. British Columbia Ministry of Energy and Mines, pp. 51–55.

Beard, J.S., and Lofgren, G.E. 1991. Dehydration melting and water-saturated melting of basaltic and andesitic greenstones and amphibolites at 1, 3, and 6.9 kb. Journal of Petrology, **32**: 365–401.

Brenan, J.M., Shaw, H.F., Phinney, D.L., and Ryerson, F.J. 1994. Rutile-aqueous fluid partitioning of Nb, Ta, Hf, Zr, U and Th: implications for high field strength element depletions in island-arc basalts. Earth and Planetary Science Letters, **128**(3–4): 327–339. doi:10.1016/0012-821X(94)90154-6.

Childe, F.C., and Thompson, J.F.H. 1997. Geological setting, U–Pb geochronology, and radiogenic isotopic characteristics of the Permo-Triassic Kutcho Assemblage, north-central British Columbia. Canadian Journal of Earth Sciences, **34**: 1310–1324. doi:10.1139/e17-104.

Childe, F.C., Thompson, J.F.H., Mortenson, J.K., Friedman, R.M., Schiarizza, P., Bellefontaine, K., and Marr, J.M. 1998. Primitive Permo-Triassic volcanism in the Canadian Cordillera: tectonic and metallogenic implications. Economic Geology and the Bulletin of the Society of Economic Geologists, **93**: 224–231.

Cloos, M. 1993. Lithospheric buoyancy and collisional orogenesis: Subduction of oceanic plateaus, continental margins, island arcs, spreading ridges, and seamounts. Geological Society of America Bulletin, **105**(6): 715–737. doi:10.1130/0016-7606(1993)105<0715:LBACOS>2.3.CO;2.

Colpron, M., and Friedman, R.M. 2008. U–Pb zircon ages for the Nordenskiold formation (Laberge Group) and Cretaceous intrusive rocks, Whitehorse Trough, Yukon. *In* Yukon exploration and geology 2007. Yukon Geological Survey, pp. 139–151.

Coney, P.J., Jones, D.L., and Monger, J.W.H. 1980. Cordilleran suspect terranes. Nature, **288**(5789): 329–333. doi:10.1038/288329a0.

Cordey, F., Gordey, S.P., and Orchard, M.J. 1991. New biostratigraphic data from the northern Cache Creek terrane, Teslin map area, southern Yukon. *In* Current research part E. Geological Survey of Canada, pp. 67–76.

Cox, K.G., Bell, J.D., and Pankhurst, R.J. 1979. The interpretation of igneous rocks. George Allen and Unwin, London, UK.

Devine, F.A.M. 2002. U–Pb geochronology, geochemistry, and tec-

Fig. 11. Comparison of Nakina lithogeochemical data (shaded area) with other data from the northern Cache Creek terrane using (*a*) the Th–Hf–Nb tectonic discrimination diagram (after Wood 1980); (*b*) a Th/Yb versus Nb/Yb diagram (modified from Pearce et al. 1995; Metcalf et al. 2000); (*c*) chondrite-normalized rare-earth element (REE) plots using the normalizing values of Taylor and McLennan (1985); and (*d*) trace-element spider diagrams normalized to normal mid-ocean ridge basalt (N-MORB) using the values from Sun and McDonough (1989). Data from the Hall Lake, French Range, and Kutcho Creek areas are from Mihalynuk and Cordey (1997).

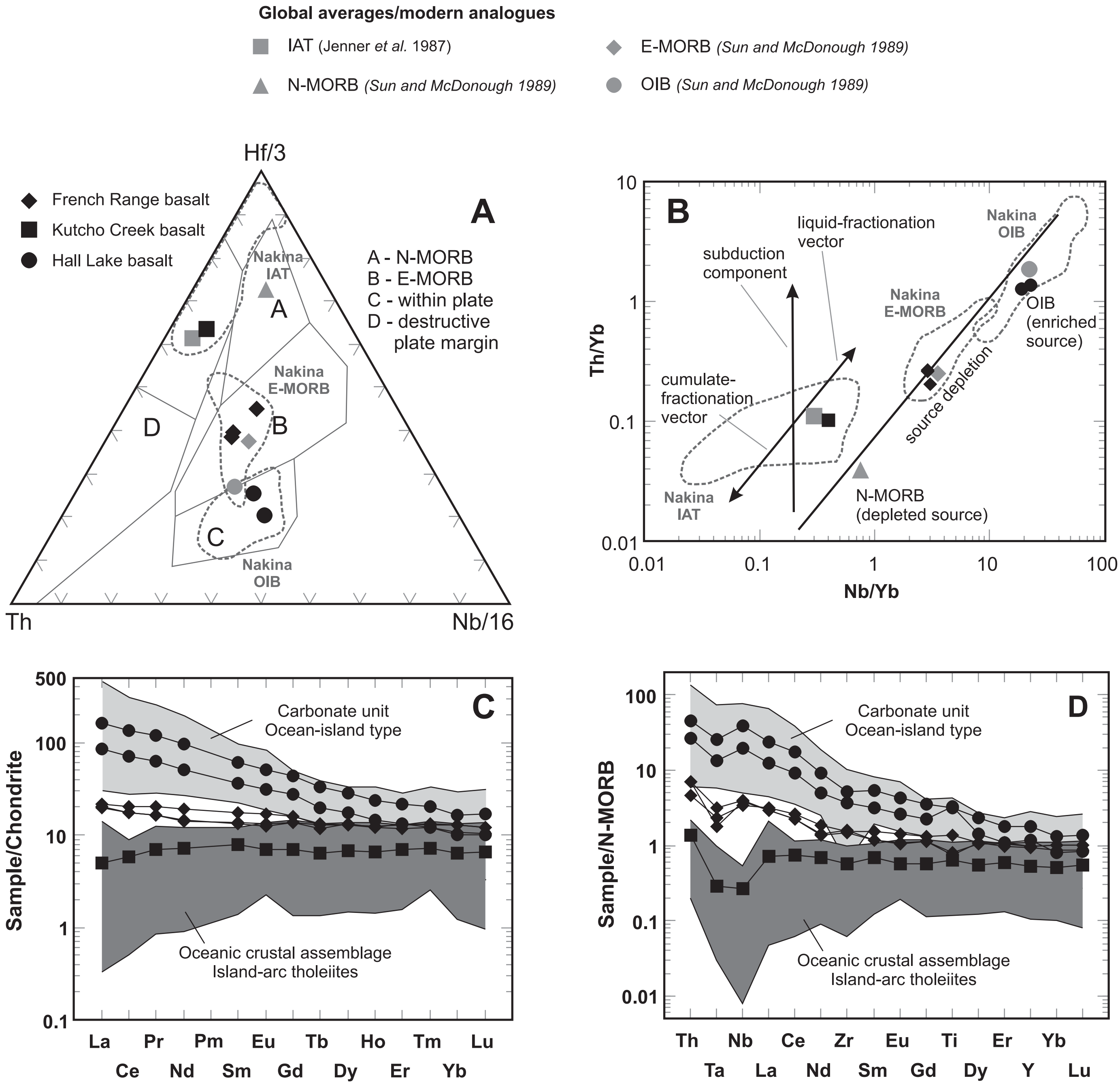

tonic implications of oceanic rocks in the northern Cache Creek Terrane, Nakina area, northwestern British Columbia. B.Sc. thesis, The University of British Columbia, Vancouver, B.C.

English, J.M., and Johnston, S.T. 2005. Collisional orogenesis in the northern Canadian Cordillera: Implications for Cordilleran crustal structure, ophiolite emplacement, continental growth, and the terrane hypothesis. Earth and Planetary Science Letters, **232**(3–4): 333–344. doi:10.1016/j.epsl.2005.01.025.

English, J.M., Mihalynuk, M.G., Johnston, S.T., and Devine, F.A.M. 2002. Atlin TGI Part III: Geology and petrochemistry of mafic rocks within the northern Cache Creek terrane and tectonic implications. *In* Geological fieldwork 2001. British Columbia Ministry of Energy and Mines, pp. 19–30.

English, J.M., Johannson, G.G., Johnston, S.T., Mihalynuk, M.G., Fowler, M., and Wight, K.L. 2005. Structure, stratigraphy and hydrocarbon potential of the central Whitehorse Trough, northern Canadian Cordillera. Bulletin of Canadian Petroleum Geology, **53**(2): 130–153. doi:10.2113/53.2.130.

Gabrielse, H. 1998. Geology of Cry Lake and Dease Lake map areas, north-central British Columbia. Geological Survey of Canada, Bulletin 504.

Gordey, S.P., McNicoll, V.J., and Mortenson, J.K. 1998. New U–Pb ages from the Teslin area, southern Yukon, and their bearing on terrane evolution in the northern Cordillera. *In* Radiogenic age and isotopic studies. Geological Survey of Canada, pp. 129–148.

Green, T.H., and Pearson, N.J. 1987. An experimental study of Nb and Ta partitioning between Ti-rich minerals and silicate liquids at high pressure and temperature. Geochimica et Cosmochimica Acta, **51**(1): 55–62. doi:10.1016/0016-7037(87)90006-8.

Haase, K.M., Stroncik, N.A., Hekinian, R., and Stoffers, P. 2005. Nb-depleted andesites from the Pacific–Antarctic Rise as analogs for early continental crust. Geology, **33**(12): 921–924. doi:10.1130/G21899.1.

Hart, C.J.R. 1996. Magmatic and tectonic evolution of the Intermontane superterrane and Coast Plutonic Complex in souterhn Yukon Territory. M.Sc. thesis, The University of British Columbia, Vancouver, B.C.

Isozaki, Y., Maruyama, S., and Furuoka, F. 1990. Accreted oceanic materials in Japan. Tectonophysics, **181**(1–4): 179–205. doi:10.1016/0040-1951(90)90016-2.

Jenner, G.A. 1996. Trace element geochemistry of igneous rocks: geochemical nomenclature and analytical geochemistry. *In* Trace element geochemistry of volcanic rocks: applications for massive sulphide exploration. *Edited by* D.A. Wyman. Geological Association of Canada. Short Course Notes, pp. 51–77.

Jenner, G.A., Cawood, P.A., Rautenschlein, M., and White, W.M. 1987. Composition of back-arc basin volcanics, Valu Fa Ridge, Lau Basin: evidence for a slab-derived component in their mantle source. Journal of Volcanology and Geothermal Research, **32**(1–3): 209–222. doi:10.1016/0377-0273(87)90045-X.

Jenner, G.A., Longerich, H.P., Jackson, S.E., and Fryer, B.J. 1990. ICP–MS — A powerful tool for high-precision trace-element analysis in Earth sciences: evidence from analysis of selected U.S.G.S. reference samples. Chemical Geology, **83**(1–2): 133–148. doi:10.1016/0009-2541(90)90145-W.

Johannson, G.G., Smith, P.L., and Gordey, S.P. 1997. Early Jurassic evolution of the northern Stikinian arc: evidence from the Laberge Group, northwestern British Columbia. Canadian Journal of Earth Sciences, **34**: 1030–1057. doi:10.1139/e17-085.

Merran, Y. 2002. Mise en place et environment de depot d'une plate-forme carbonatee intraoceanique: example du complexe d'Atlin, Canada. M.Sc. thesis, Université Claude Bernard, France.

Metcalf, R.V., Wallin, E.T., Willse, K.R., and Muller, E.R. 2000. Geology and geochemistry of the ophiolitic Trinity terrane, California: Evidence of middle Paleozoic depleted supra-subduction zone magmatism in a proto-arc setting. *In* Ophiolites and oceanic crust: new insights from field studies and the ocean drilling program. *Edited by* Y. Dilek, E.M. Moores, D. Elthon, and A. Nicolas. Geological Society of America, Boulder, Colo., pp. 403–418.

Mihalynuk, M.G 1999. Geology and mineral resources of the Tagish Lake area (NTS 104M/8, 9, 10E, 15 and 104N/12W) northwestern British Columbia. British Columbia Ministry of Energy, Mines and Petroleum Resources, Bulletin 105.

Mihalynuk, M.G., and Cordey, F. 1997. Potential for Kutcho Creek volcanogenic massive sulphide mineralization in the northern Cache Creek terrane: a progress report. *In* Geological fieldwork 1996. British Columbia Ministry of Employment and Investment, pp. 157–170.

Mihalynuk, M.G., Smith, M.T., Gabites, J.E., Runkle, D., and Lefebure, D. 1992. Age of emplacement and basement character of the Cache Creek terrane as constrained by new isotopic and geochemical data. Canadian Journal of Earth Sciences, **29**: 2463–2477. doi:10.1139/e92-193.

Mihalynuk, M.G., Johnston, S.T., Lowe, C., Cordey, F., English, J.M., Devine, F.A.M., Larson, K., and Merran, Y. 2002. Atlin TGI Part II: Preliminary results from the Atlin Targeted Geoscience Initiative, Nakina area, northwest British Columbia. *In* Geological fieldwork 2001. British Columbia Ministry of Energy and Mines, pp. 5–18.

Mihalynuk, M.G., Johnston, S.T., English, J.M., Cordey, F., Villeneuve, M.E., Rui, L., and Orchard, M.J. 2003*a*. Atlin TGI, Part II: Regional geology and mineralization of the Nakina area (NTS 104N/2W and 3). *In* Geological fieldwork 2002. British Columbia Ministry of Energy and Mines, pp. 9–37.

Mihalynuk, M.G., Villeneuve, M.E., and Cordey, F. 2003*b*. Atlin TGI, Part III: Geological setting and style of mineralisation at the Joss'alun Occurrence, Atlin area (NTS 104N/2SW), MINFILE 104N136. *In* Geological fieldwork 2002. British Columbia Ministry of Energy and Mines, pp. 39–49.

Mihalynuk, M.G., Erdmer, P., Ghent, E.D., Cordey, F., Archibald, D., Friedman, R.M., and Johannson, G.G. 2004*a*. Subduction to obduction of coherent French Range blueschist — in less than 2.5 Myrs? Geological Society of America Bulletin, **116**: 910–922. doi:10.1130/B25393.1.

Mihalynuk, M.G., Fiererra, L., Robertson, S., Devine, F.A.M., and Cordey, F. 2004*b*. Geology and new mineralisation in the Joss'alun belt, Atlin area. *In* Geological fieldwork 2003. British Columbia Ministry of Energy and Mines, pp. 61–82.

Monger, J.W.H. 1969. Stratigraphy and structure of Upper Paleozoic rocks, northeast Dease Lake map-area, British Columbia (104J). Geological Survey of Canada, Paer 68-48.

Monger, J.W.H. 1975. Upper Paleozoic rocks of the Atlin terrane. Geological Survey of Canada, Paper 74-47.

Monger, J.W.H. 1977. Upper Paleozoic rocks of the northwestern British Columbia. Geological Survey of Canada, Paper 77-1A, pp. 255–262.

Monger, J.W.H., and Ross, C.A. 1971. Distribution of fusulinaceans in the western Canadian Cordillera. Canadian Journal of Earth Sciences, **8**: 259–278. doi:10.1139/e71-026.

Monger, J.W.H., Price, R.A., and Tempelman-Kluit, D.J. 1982. Tectonic accretion and the origin of the two major metamorphic and plutonic welts in the Canadian Cordillera. Geology, **10**(2): 70–75. doi:10.1130/0091-7613(1982)10<70:TAATOO>2.0.CO;2.

Nicolas, A. 1995. The mid-oceanic ridges: mountains below sea-level. Springer Verlag, Heidelberg, Germany.

Nicolas, A., and Violette, J.F. 1982. Mantle flow at oceanic spreading centres: models derived from ophiolites. Tectonophysics, **81**(3–4): 319–339. doi:10.1016/0040-1951(82)90136-6.

Orchard, M.J. 1991. Conodonts, time and terranes: An overview of the biostratigraphic record in the western Canadian Cordillera. *In* Ordovician to Triassic conodont palaeontology of the Canadian Cordillera. *Edited by* M.J. Orchard, and A.D. McCracken. Geological Survey of Canada, pp. 1–25.

Orchard, M.J., Struik, L.C., Rui, L., Bamber, E.W., Mamet, B., Sano, H., and Taylor, H. 2001. Palaeontological and biogeographical constraints on the Carboniferous to Jurassic Cache Creek terrane in central British Columbia. Canadian Journal of Earth Sciences, **38**: 551–578. doi:10.1139/cjes-38-4-551.

Pearce, J.A. 1982. Trace element characteristics of lavas from destructive plate boundaries. *In* Orogenic andesites and related rocks. *Edited by* R.S. Thorpe. John Wiley & Sons, Chichester, UK, pp. 525–548.

Pearce, J.A. 1996. A user's guide to basalt discrimination diagrams.

In Trace element geochemistry of volcanic rocks: applications for massive sulphide exploration. *Edited by* D.A. Wyman. Geological Association of Canada, Short Course Notes, pp. 79–113.

Pearce, J.A., and Peate, D.W. 1995. Tectonic implications of the composition of volcanic arc magmas. Annual Review of Earth and Planetary Sciences, **23**(1): 251–285. doi:10.1146/annurev.ea.23.050195.001343.

Pearce, J.A., Baker, P.E., Harvey, P.K., and Luff, I.W. 1995. Geochemical evidence for subduction fluxes, mantle melting and fractional crystallization beneath the South Sandwich island arc. Journal of Petrology, **36**: 1073–1104.

Ricketts, B.D., Evenchick, C.A., Anderson, R.G., and Murphy, D.C. 1992. Bowser basin, northern British Columbia: constraints on the timing of initial subsidence and Stikinia — North America terrane interactions. Geology, **20**(12): 1119–1122. doi:10.1130/0091-7613(1992)020<1119:BBNBCC>2.3.CO;2.

Rudnick, R.L., and Fountain, D.M. 1995. Nature and composition of the continental crust: a lower crustal perspective. Reviews of Geophysics, **33**(3): 267–309. doi:10.1029/95RG01302.

Rudnick, R.L., Barth, M., Horn, I., and McDonough, W.F. 2000. Rutile-bearing refractory eclogites: Missing link between continents and depleted mantle. Science, **287**(5451): 278–281. doi:10.1126/science.287.5451.278.

Ryerson, F.J., and Watson, E.B. 1987. Rutile saturation in magmas: implications for Ti–Nb–Ta depletion in island-arc basalts. Earth and Planetary Science Letters, **86**(2–4): 225–239. doi:10.1016/0012-821X(87)90223-8.

Schiarizza, P., Massey, N., MacIntyre, D.G., and Villeneuve, M.E. 2000. The Sitlika Assemblage, west-central Cache Creek terrane, British Columbia: Primitive Permo-Triassic and subsequent Triassic–Jurassic clastic overlap assemblage. *In* Abstracts with Programs. Geological Society of America, Paper 67.

Smith, R.E., and Smith, S.E. 1976. Comments on the use of Ti, Zr, Y, Sr, K, P and Nb in classification of basalt. Earth and Planetary Science Letters, **32**(2): 114–120. doi:10.1016/0012-821X(76)90049-2.

Souther, J.G. 1971. Geology and mineral deposits of Tulsequah map-area, British Columbia. Geological Survey of Canada, Memoir 362.

Sun, S., and McDonough, W.F. 1989. Chemical and isotopic systematics of oceanic basalts: implications for mantle composition and processes. *In* Magmatism in the ocean basins. *Edited by* A.D. Saunders, and N.J. Norry. Geological Society of London, pp. 313–345.

Taylor, S.R., and McLennan, S.M. 1985. The continental crust: Its composition and evolution. Blackwell Scientific, Boston, Mass.

Terry, J. 1977. Geology of the Nahlin ultramafic body, Atlin and Tulsequah map-areas, northwestern British Columbia. *In* Current research. Geological Survey of Canada, pp. 263–266.

Thorstad, L.E., and Gabrielse, H. 1986. The Upper Triassic Kutcho Formation, Cassiar Mountains, north-central British Columbia. Geological Survey of Canada, Paper 86-16.

Walker, J.D., and Geissman, J.W. 2009. 2009 GSA Geologic Time Scale. Geological Society of America Today, **19**: 60–61.

Winchester, J.A., and Floyd, P.A. 1977. Geochemical discrimination of different magma series and their differentiation products using immobile elements. Chemical Geology, **20**: 325–343. doi:10.1016/0009-2541(77)90057-2.

Wood, D.A. 1980. The application of a Th–Hf–Ta diagram to problems of tectonomagmatic classification and to establishing the nature of crustal contamination of basaltic lavas of the British Tertiary volcanic province. Earth and Planetary Science Letters, **50**(1): 11–30. doi:10.1016/0012-821X(80)90116-8.